Mathematical framework on correlation function and conditional yield in $d-Au$ and $p-p$

Jiangyong Jia,Brian Cole

July 14, 2004

Abstract

In this short note, we discuss the mathematic framework of two particle correlation in $\Delta\phi$ and $\Delta\eta$ space. In contrast to the previous analysis by Paul Stankus[1] which focused on simplified one dimensional correlation function and ideal acceptance, we derived formulas suitable for detector with limited acceptance, and for both two dimensional($\Delta\phi$ and $\Delta\eta$) and one dimensional($\Delta\phi$ or $\Delta\eta$) correlation functions. The validity of our formulas are confirmed with Monte Carlo simulations.

Contents

1 Introduction

In heavy-ion collisions, due to the large amount of soft background ($>$ 300 GeV/srad in central Au-Au collisions), it is very difficult to directly reconstruct jets using the standard method[2, 3]. Even in the dAu or pp collisions, the range of energy accessible to direct jet reconstruction is limited to $p_T > 10$ GeV (star). The situation is even more complicated for finite acceptance detectors like PHENIX. Considering a typical hadron from a jet pointing inside the PHENIX η acceptance, it's average angle from jet direction is $\langle\theta\rangle \approx \langle j_T\rangle / p \approx 0.4/p$. Thus the size of the jet cone is inversely proportional to the particle momentum, and at given momentum, only a certain fraction of the fragmented hadrons would fall within the acceptance. To improve the situation, a fiducial cut technique is often used where the jet direction is required to be far from the edge of the detector acceptance. For example, we can select only the jets within $|\eta| < 0.15$ in PHENIX to increase the acceptance for low p_T fragments. In this case, the associated hadrons with $p > 2(4) GeV/c$ would have more than 68% (93%) probability to fall within the PHENIX acceptance(assuming j_T distribution is gauss). However, the benefit of this technique is limited, for a 20 GeV jet within the fiducial window, a significant fraction of soft fragments ($z < 0.1$) would still fall outside the PHENIX acceptance. In addition, it also leads to the uncertainties in determining the jet direction.

Two-particle-correlation technique provides an alternative way to measure the properties of the jet. It is based on the fact that the fragments are tightly correlated in azimuth ϕ and pseudo-rapidity η and the jet signal will manifest itself as a narrow peak in $\Delta\phi$ and $\Delta\eta$ space. This method was widely used in 70's at several experiments in searching for jet signal in $p-p$ collisions at CERN ISR. One of Mike Tannenbaum's favorite two particle correlation plot is shown in Fig.1, the typical back-to-back structure in two particle correlation is clearly visible. The interesting quantity directly connects to the underling hard scattering process is the dihadron correlation function,

$$D_{h_1h_2}(p_{T,trig}, p_{T,asso}) = \frac{d\sigma_{AB}^{h_1h_2}/d^3p_{T,trig}d^3p_{T,asso}}{d\sigma_{AB}^{h_1}/d^3p_{T,trig}} \tag{1}$$

If both particles are from the same jet, then this function would be related to the two-hadron fragmentation function[4]. If the two particles are from back-to-back jets, then this function more or less represents the away side jet fragmentation function. Experimentally, the quantity that we measures is called the conditional yield,

$$\frac{1}{N_{trig}}\frac{d^2N}{d\Delta\phi d\Delta\eta} \tag{2}$$

Where, N_{trig} is the number of trigger particles, and $\frac{d^2N}{d\Delta\phi d\Delta\eta}$ is the number of jet pairs in a fixed $\Delta\phi$ and $\Delta\eta$ bin. The conditional yield is equivalent to the Eq.1:

$$N_{trig} \propto d\sigma_{AB}^{h_1}/d^3p_{T,trig} \tag{3}$$

$$\frac{d^2N}{d\Delta\phi d\Delta\eta} \propto d\sigma_{AB}^{h_1h_2}/d^3p_{T,trig}d^3p_{T,asso} \tag{4}$$

,

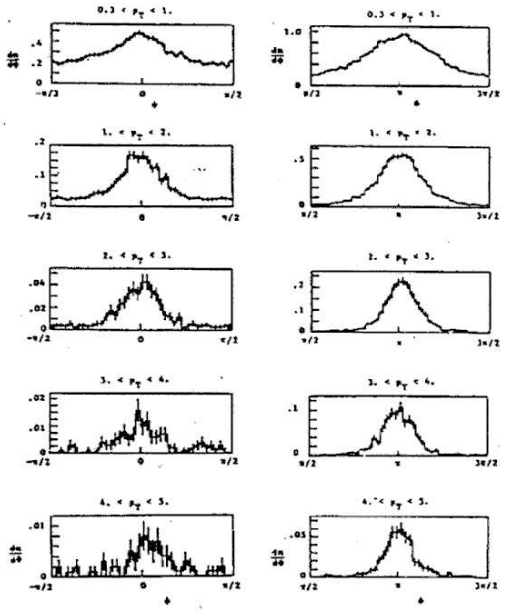

Figure 2: CCOR measurement of two particle correlations in azimuth: azimuthal distributions of charged particles as a function of their transverse momentum p_T are plotted relative to a triggering neutral with $p_{Tt} \geq 7.0$ GeV/c which defines the zero of azimuth, $\phi = 0$.

Figure 1: .

The two particle correlation technique extracts the jet fragmentation function on a statistical basis, and is more robust in dealing with the underling soft background and the limited detector acceptance. In PHENIX, we estimate both effects using event mixing technique. This technique was frequently used in resonance or two particle interferometry, and was proved to be very reliable in extracting small signal from large background.

Our goal of two particle correlation (or jet correlation) study is to measure the properties of jet fragmentation: 1) the width of the correlation function, which reflects the jet fragmentation momentum j_T and parton transverse momentum k_T. 2) the yield of hadrons associated with jet as function of hadron momentum along the jet axis, which is directly connected with the fragmentation function. This note is organized in several sections, in Section2 we shall discuss estimation of background and pair acceptance using event mixing technique. In Section3 and 4, we shall discuss on a general ground the two particle correlation function, and its reduction into two-Dimensional and one-Dimensional correlation functions. In the end of Section 4, we derive the correction factor for the jet conditional yield. Finally in Section.5, we discuss the normalization of event mixing background, and test our formulas using simple Monte-Carlo and Pythia simulation.

2 Jet correlation

2.1 Event mixing technique

In general, any pair distributions constructed from the same event are composed of two parts: the signal pairs and the background pairs. Collectively, these pairs are called the foreground pairs. For our purpose, the signal pairs specifically refer to the pairs coming from the same jet; while the background pairs could include pairs from soft particles, pairs by combine one soft particle with one jet particle and also pairs by combining two jet particles from two different hard scattering processes. To estimate the background contribution, the event mixing technique is used, where the mix pair distribution is constructed by combining particle 1 and 2 picked out of two different events. The idea behind this method is that this mixed pair distributions contain all the effects of the event and the detectors except the correlation of interest.

Event mixing technique has been tried in the study of resonance production[5], HBT correlation[6, 7, 8, 9] and di-lepton production[10]. it was shown before that there are certain limitations[11, 12] which become important when the signal is small comparing to background. In jet correlation study, we have a very different scenario. The jet signal is relatively large, it can be comparable or even exceeds the background. The list of the problems associated with event-mixing in jet correlation are somewhat different from those in conventional approach. A partial list of the main issues with event mixing are: 1) normalization problem due to centrality smearing, 2) additional event multiplicity smearing due to the much larger multiplicity of jet event relative to minimum bias event, 3) resonance contamination to the jet peak, 4) distortion of the jet shape due to detector effect such as two track resolution, 5) global constraint like momentum conservation, which is important in pp and peripheral dAu etc. Some of these issues are addressed in.

Generally speaking, the problems we face in jet correlation are simpler than that for dihadron, HBT, or di-lepton mass spectra. Because of the large signal in jet correlation, many of the problems inherent in the small signal to background ratio become irrelevant. More importantly, the underling background distribution is almost flat in $\Delta\phi$ and $\Delta\eta$, in contrast to a rapidly varying mass distribution. The additional non-flatness imposed by detector acceptance, multiplicity smearing, and other effects can be estimated rather reliably .

Let's denote the single particle acceptance as Ω. As example, Fig.2 shows the nominal PHENIX acceptance in ϕ and η [1]. The pair acceptance is $\Omega \otimes \Omega$, which, when projected onto the relative variable $\Delta\phi = \phi_2 - \phi_1$ and $\Delta\eta = \eta_2 - \eta_1$, is not uniform(see Section.3.1). One of the advantage of using event mixing technique in jet correlation is that the mix pair distribution naturally includes the finite detector acceptance, and we can use the shape of the mix distribution(pair acceptance function) in $\Delta\phi$ and $\Delta\eta$ to correct the acceptance loss in the signal pair distribution. There is a simple sum rule which shows that the integral of pair acceptance function in $\Delta\phi$ and $\Delta\eta$ is same as the product of the two single particle acceptance function(discussed in next section). Since the particles in foreground pairs have the same single particle acceptance as the particles in the mixed pair, the pair acceptance function

[1] Since the η coverage is rather small, the difference between polar angle θ and pseudo-rapidity is negligible. η can be replaced with θ in almost all formula derived.

should be the same for foreground pair and mixed pair. Thus dividing the foreground distribution by the mix distribution should give us the pair efficiency corrected foreground distribution.

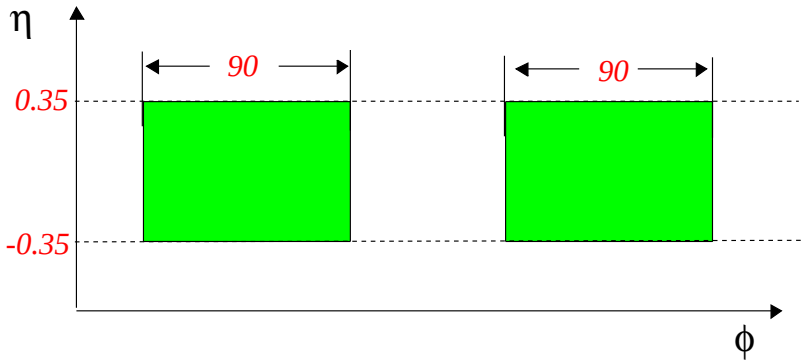

Figure 2: The PHENIX acceptance for single particle.

2.2 Sum rule for the mix pair distribution

We shall follow the derivation procedure similar to that for the like-sign method[12, 10, 13]. In a given event, assume we want to correlate two types of particles and we denoting them as type 'a' and type 'b'. In our particular case, type 'a' would be the trigger particle and type 'b' is the associated particle. These two types of particles can be non-overlapping such as correlating two particles in non-overlapping p_T ranges(we call it assorted correlation), but they can also be overlapping such as correlating two particle in the same p_T ranges (fixed correlation), in which case, type 'a' and 'b' are identical.

In the event mixing, we combine all type 'a' particles, n_a, with all type 'b' particles, n_b, from a random selected minimum bias event. Further, since the number n_a and n_b are not correlated, the probability to observe them can be factorized [2]:

$$P(n_a, n_b) = P(n_a) \times P(n_b). \tag{5}$$

Due to the limited acceptance, PHENIX can only detects a certain fraction of particles from the collision. The probability of measuring $n_a(n_b)$ out of $N_a(N_b)$ initially produced particles follows a binomial distribution $B(N_a, n_a, \epsilon_a)(B(N_b, n_b, \epsilon_b))$,

$$\begin{aligned} B(N_a, n_a, \epsilon_a) &= \frac{N_a!}{n_a!(N_a - n_a)!}\epsilon_a^{n_a}(1-\epsilon_a)^{N_a - n_a} \\ B(N_b, n_b, \epsilon_b) &= \frac{N_b!}{n_b!(N_b - n_b)!}\epsilon_b^{n_b}(1-\epsilon_b)^{N_b - n_b} \end{aligned} \tag{6}$$

[2]This subsequently would be our definition of independence (or no correlation) between two number.

where $\epsilon_a(\epsilon_b)$ is the measurement efficiency for type a(b) particles. Obviously for fixed N_a,

$$\langle n_a \rangle \mid_{N_a} = \epsilon_a N_a \quad , \left\langle (n_a - \langle n_a \rangle)^2 \right\rangle \mid_{N_a} = \epsilon_a (1 - \epsilon_a) N_a. \tag{7}$$

The measured pair distribution is

$$n_{aa} = K_{aa} \frac{n_a(n_a - 1)}{2} B(N_a, n_a, \epsilon_a) \tag{8}$$

where K_{aa} is the probability of surviving each other under the condition that each has survived the measurement for the full event(pair efficiency). K_{aa} may be less than 1 due to detector effects like two track resolution or can just come from additional pair cuts in the analysis. An good discussion on the pair efficiency can be found in [10, 12, 13].

To derive $\langle n_{aa} \rangle$, we take the properly weighted sum over all possible initial events, (N_a,N_b), weighted by the multiplicity distribution $P_a(N_a)$ and $P_b(N_b)$:

$$\begin{aligned} \langle n_{aa} \rangle &= K_{aa} \sum_{N_a} \sum_{n_a} \frac{n_a(n_a - 1)}{2} B(N_a, n_a, \epsilon_a) P_a(N_a) \\ &= \frac{1}{2} K_{aa} \epsilon_a^2 \sum_{N_a} N_a(N_a - 1) P_a(N_a) \end{aligned} \tag{9}$$

If N_a follows Poisson distribution, one can show that n_{aa} also follows Poisson distribution, and we reach a simplified result:

$$\langle n_{aa} \rangle = \frac{1}{2} K_{aa} \epsilon_a^2 \langle N_a \rangle^2 = \frac{1}{2} K_{aa} \langle n_a \rangle^2 \tag{10}$$

$$\langle n_{bb} \rangle = \frac{1}{2} K_{bb} \epsilon_b^2 \langle N_b \rangle^2 = \frac{1}{2} K_{bb} \langle n_b \rangle^2 \tag{11}$$

the number of pair between a and b particles are:

$$\begin{aligned} \langle n_{ab} \rangle &= K_{ab} \sum_{N_a, N_b} P_a(N_a) P_b(N_b) (\sum_{n_a, n_b} n_a n_b B(n_a) B(n_b)) \\ &= K_{ab} \epsilon_a \epsilon_b \sum_{N_a, N_b} N_a N_b P_a(N_a) P_b(N_b) \\ &= K_{ab} \epsilon_a \epsilon_b \langle N_a \rangle \langle N_b \rangle \\ &= K_{ab} \langle n_a \rangle \langle n_b \rangle \end{aligned} \tag{12}$$

Eq.10 - Eq.12 are the sum rules of the mix pairs. It gives the relation between the total number of pairs and total number of singles. **NOTE:** Relation Eq.10 (or Eq.11) is the sum rule for fixed p_T correlation, it requires only the poisson assumption on the underlying multiplicity. On the other hand, Eq.12, which is the sum rule for assorted p_T correlation, requires only the statistical independence (Eq.5) of type 'a' and type 'b'.

Under the assumption that $K_{ab} = \sqrt{K_{aa}K_{bb}}$, we have

$$\langle n_{ab} \rangle = 2\sqrt{\langle n_{aa} \rangle \langle n_{bb} \rangle} \tag{13}$$

Assuming we measured N_{evt} events, we find that the total integral of the combinatorial pairs have following relation,

$$\langle N_{ab} \rangle = 2\sqrt{\langle N_{aa} \rangle \langle N_{bb} \rangle} \tag{14}$$

This relation was frequently used in the like sign background subtraction method for dilepton invariant mass distribution in CERES[14]. This relation requires one to calculate the type 'a' and type 'b' pairs within the same event, and the normalization of the determined background to signal+background is straight forward. Unfortunately, as we will discuss in next section, this method is not suitable for estimation of the background in jet correlation because of the dominance of signal and the breakdown of poisson assumption.

2.3 Different types of jet correlations in PHENIX

Currently in $d - Au$ and $p - p$, there are following different jet correlation analysis.

1. low p_T trigger

   - fixed p_T charged-charged correlation[Nathan], both trigger and associated particle p_T are below 4.5 GeV/c
   - assorted p_T charged-charged correlation[Wolf,Anne], typical trigger is $2.5 < p_{T,trig} < 4.5$ GeV/c and typical associated particle is $1 < p_{T,asso} < 2.5$ GeV/c
   - Central arm and muon arm correlation [Chun]

2. intermediate p_T trigger

   - assorted p_T γ- charged correlation[Mickey], typical trigger is $p_{T,trig} > 3.5$ GeV/c, associated $p_{T,asso} < 4$ GeV/c

3. high p_T trigger

   - assorted p_T $\pi^{\pm}$-charged correlation[Jiangyong], typical trigger is $5 < p_{T,trig} < 16$ GeV/c, associated $0.4 < p_{T,asso} < 5$ GeV/c.
   - assorted p_T π^0-charged correlation[Nathan,Jan], typical trigger is $5 < p_{T,trig} < 10$ GeV/c, associated $2 < p_{T,asso} < 5$ GeV/c.

In principle, different analysis use more or less the same technique. However, there are different difficulties associated with each analysis are driven by different statistics and slightly different underling physics. In general, the amount of background and resonance contamination become more significant as one decrease the trigger p_T, the acceptance correction also become bigger. On the other hand high p_T trigger correlation often suffers from limited

statistics and special care need to be employed in the fitting procedure to handle correctly the errors.

To simplify the discussion, we shall use $\pi^{\pm}$-charged hadron correlation as example in following sections. We will come back in Section, to discuss the differences in other analysis.

2.4 Separating the signal and the background

If the mixed pair distribution can reproduce the background, the difference between the original events and the mixed events distributions would represent the signal only. The main goal of this section is to find out to what level the mix pair [3] rate from event mixing can match the true background in foreground pair distribution.

In general, both trigger and associated particles can contain both signal and background particles. Further, we assume that there are no correlations between the signal and background particles and also no correlations among the background particles. The signal that we are interested in include pairs from same jets, which peaks at small $\Delta\phi$ and $\Delta\eta$(near side or same side) and back-to-back jets, which peaks at $\Delta\phi = \pi$(far side or away side). For simplicity, in the following, we discuss only the assorted correlation, and also consider only pair distribution for the near side. Similar formula can be derived for fixed p_T correlation and also the away side.

In the case of foreground, when we make pairs out of an event, we have following five cases, each with total number of pairs $n_{ab}^{fg,i}$ ($i = 1$ to 5),

1. 'a' and 'b' both from background, $n_{ab}^{fg,1} = n_a n_b$.
2. 'a' from background and 'b' from jet, $n_{ab}^{fg,2} = n_a n_{jet} \left\langle n_b^{jet} \right\rangle$.
3. 'b' from background and 'a' from jet, $n_{ab}^{fg,3} = n_{jet} \left\langle n_a^{jet} \right\rangle n_b$.
4. 'a' and 'b' are from different jets, $n_{ab}^{fg,4} = n_{jet}(n_{jet} - 1) \left\langle n_a^{jet} \right\rangle \left\langle n_b^{jet} \right\rangle$.
5. 'a' and 'b' are from the same jets, $n_{ab}^{fg,5} = n_{jet} \left\langle n_a^{jet} n_b^{jet} \right\rangle$

n_a, n_{jet} and $\langle n_a^{jet} \rangle$ are the number of type 'a' background particles per event, the number of jets per event and the average number of type 'a' particles per jet in one event, respectively. Among these five terms, only $n_{ab}^{fg,5}$ represents the signal that we want to extract, all other four terms contribute to the background:

$$n_{ab,bg}^{fg} = n_a n_b + n_a n_{jet} \left\langle n_b^{jet} \right\rangle + n_{jet} \left\langle n_a^{jet} \right\rangle n_b + n_{jet}(n_{jet} - 1) \left\langle n_a^{jet} \right\rangle \left\langle n_b^{jet} \right\rangle \tag{15}$$

In the event mixing, we typically mix the the trigger with charged particles from a randomly selected minimum bias event with the similar centrality and vertex. There are four terms, each with total number of pairs $n_{ab}^{mix,i}$ ($i = 1$ to 4), that contributes to the mix pairs,

1. 'a' and 'b' both from background, $n_{ab}^{mix,1} = n_a n_b'$.

[3] sometimes we also call it the combinatoric pair

2. ‘a‘ from background and ‘b‘ from jet, $n_{ab}^{mix,2} = n_a n'_{jet} \left\langle n_b^{jet\prime} \right\rangle$.

3. ‘b‘ from background and ‘a‘ from jet, $n_{ab}^{mix,3} = n_{jet} \left\langle n_a^{jet} \right\rangle n'_b$.

4. ‘a‘ and ‘b‘ are from different jets, $n_{ab}^{mix,4} = n_{jet} n'_{jet} \left\langle n_a^{jet} \right\rangle \left\langle n_b^{jet\prime} \right\rangle$

The total number of pairs are:

$$n_{ab,bg}^{mix} = n_a n'_b + n_a n'_{jet} \left\langle n_b^{jet\prime} \right\rangle + n_{jet} \left\langle n_a^{jet} \right\rangle n'_b + n_{jet} n'_{jet} \left\langle n_a^{jet} \right\rangle \left\langle n_b^{jet\prime} \right\rangle \tag{16}$$

Generally speaking, event mixing does not necessary reproduce the background level in the real events, because the rate of the associated particle in minimum bias event does not necessary equal to that in foreground event ($n'_b \neq n_b$ and $n'_{jet} \left\langle n_b^{jet\prime} \right\rangle \neq n_{jet} \left\langle n_b^{jet} \right\rangle$). Even assuming they are equal, we would still need additional assumption in order to make $n_{ab}^{fg,4} = n_{ab}^{mix,4}$ (like assuming the number of jets follows poisson statistics). As an example, Fig.3 shows the foreground and mixed pair distribution in $d-Au$ for fixed trigger p_T range and varying associated p_T ranges. The triangular shape in the mix pair distribution is characteristic of the pair acceptance function caused by the limited detector acceptance. In Fig.4, the ratio of the foreground to background from event mixing is shown. This ratio, with the pair acceptance divided out, shows the typical jet correlation peaks at the same side and away side. The combinatoric background level, derived from a double gauss plus constant fit, gives value close to 1 at low $p_{T,asso}$, but steadily increase as one increase the $p_{T,asso}$, reaching a level of 2.4 for $3 < p_{T,asso} < 4.5$ GeV/c. This increase, clearly indicates that the event mixing systematically underestimates the true background in same event pair distribution.

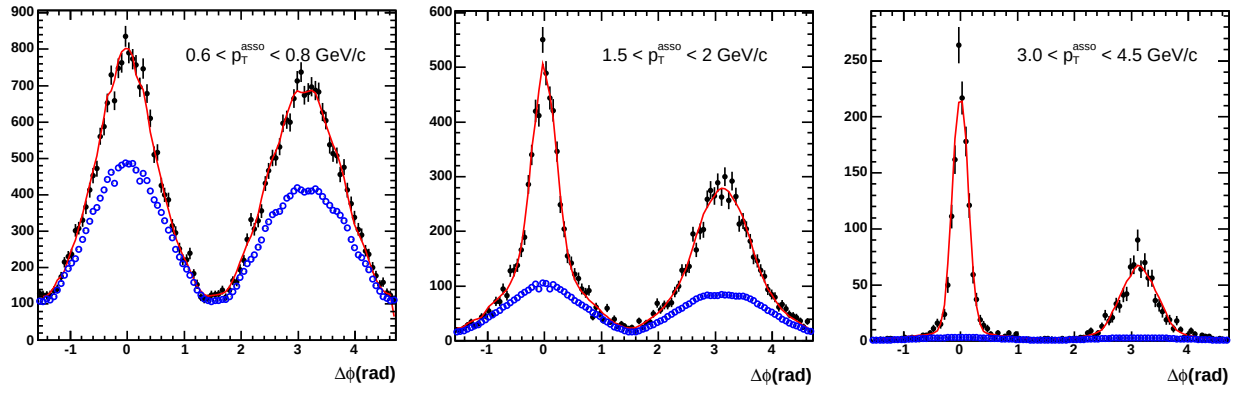

Figure 3: The same event and mix pair $\Delta\phi$ distribution for three associated (type ‘b‘) p_T ranges in $d-Au$: 0.6-0.8 GeV/c (left panel), 1.5-2 GeV/c (middle panel) and 3-4.5 GeV/c (right panel). The trigger (type ‘a‘) particles are charged pions from 5 to 10 GeV/c. The associated particles are unidentified charged hadrons. The same event pair distribution is shown by the histogram with the fit; the mix pair distribution is shown by the open circles(lower histogram).

To simply Eq.15 and Eq.16 a little bit, we consider $\pi^{\pm} - h$ case. The trigger particle (charged pion above 5 GeV/c) rate is about one per 10000 minimum bias event, the soft

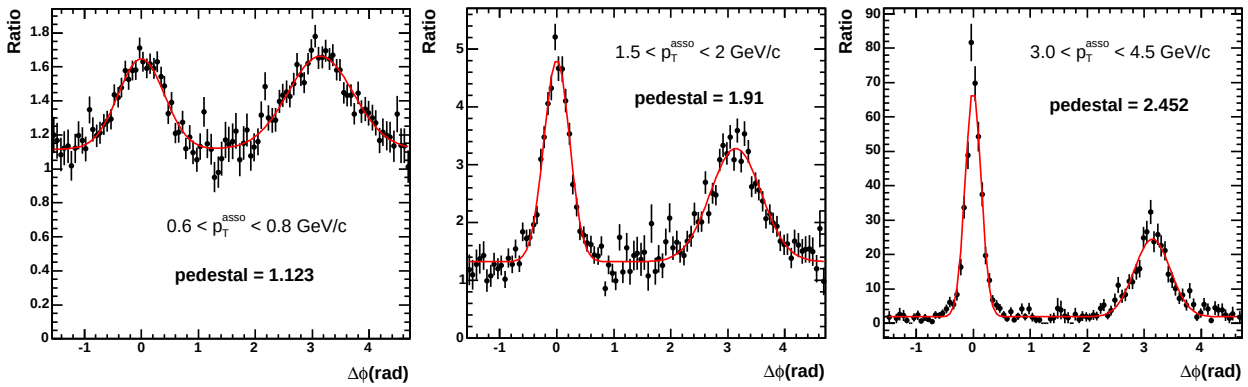

Figure 4: The ratio of same event and mix pair $\Delta\phi$ distribution for three associated (type 'b') p_T ranges in $d-Au$: 0.6-0.8 GeV/c (left panel), 1.5-2 GeV/c (middle panel) and 3-4.5 GeV/c (right panel). The trigger (type 'a') particles are charged pions from 5 to 10 GeV/c. The associated particles are unidentified charged hadrons. The constant level in the foreground relative to the mix pair, 'pedestal' is 1.123,1.91 and 2.452 for the three associated p_T, respectively.

background contribution to the trigger should be even smaller, $n_a \ll 10^{-4}$. The associated particle rate is about a few to 1000 event, $10^{-4} < n_b < 1$, depending on the $p_{T,asso}$. In the foreground event, where we require at least one trigger, the probability to have multiple jets in the same event is also high, $n^{jet} > 1$, while in the minimum bias event, this probability is small, $n^{jet\prime} \ll 1$. Based on these considerations, we can simplify Eq.15 and Eq.16 as

$$n^{fg}_{ab,bg} \approx n_{jet} \left\langle n^{jet}_a \right\rangle n_b + n_{jet}(n_{jet}-1) \left\langle n^{jet}_a \right\rangle \left\langle n^{jet}_b \right\rangle \quad (17)$$

$$n^{mix}_{ab,bg} \approx n_{jet} \left\langle n^{jet}_a \right\rangle n'_b \quad (18)$$

In both foreground and mixed pair distribution, the dominating background do not come from the soft-soft combination, but comes from hard-soft combination. Further, the fact that the background level in same event pair distribution is larger than mix pair distribution indicates that either the pure soft background level in triggered event is much larger than that in minimum bias event $n_b > n'_b$ or there are significant multi-jet production in the triggered event. Since the pure soft background drops exponentially as function of p_T, its contribution should be smaller as one increase $p_{T,asso}$. Thus we concluded that this increase must comes from the multi-jet production [4]

The main problem with event mixing is that it is very difficult to match n'_b with n_b and also $n'_{jet} \left\langle n^{jet\prime}_b \right\rangle$ with $n_{jet} \left\langle n^{jet}_b \right\rangle$. This problem is partially caused by the centrality smearing as in $d-Au$, event mixing will tends to underestimate the background level because the N_{coll} or N_{part} selected at given centrality is not poisson. However there is more to it. The fact that $p-p$ collision with jet in it can have a totally different multiplicity fluctuation(non-poisson)

[4]This can't be caused by the background in the trigger pions, because first the background in the trigger sample is well below 5%[15] and the contribution is negligible. second, the background would contribute equally to foreground and mix distribution.

than that the mix event can cause additional multiplicity smearing effect [5].

Because of the difficulty in estimating all possible multiplicity fluctuation using event mixing method, we do not intend to do an absolute normalization of background using event mixing method. Rather, we use the mix pair distribution to obtain the shape of the background distribution in $\Delta\phi$ and $\Delta\eta$, which essentially is the pair acceptance function. By dividing the same event pair distribution by the mix pair distribution, the detector acceptance effect would cancel out, and we are left with a distribution that contains a flat background plus a jet signal that has it's acceptance shape been take out[6]. The only thing left is to figure out the normalization factor. In Section.3-4, we shall give rigorously mathematical proof, accompanied by detailed MC simulation, showing that this procedure indeed gives the correct conditional yield.

3 Conditional yield in 2D

3.1 2D correlation function

In this section, we attempt to establish the formulas for the conditional yield in $\Delta\phi$ and $\Delta\eta$. Some of the ideas have been discussed in other peoples analysis note, in particular, Paul Stankus [1] and Mickey Chiu [18].

The jet signal we would like to extract from the two particle correlation function depends the relative angle between the trigger and partner particles, $\Delta\phi$ and $\Delta\eta$. The signal might also depend on the transverse momentum, p_T, centrality, N_{part}, and flavor, f, of both particles. Meanwhile, the pair acceptance function, acc, depends on ϕ, η and p_T of both particles and probably collision vertex z.

The general correlation function in PHENIX can be written as,

$$C(\phi_1,\phi_2,\eta_1,\eta_2,p_{T1},p_{T2},N_{part},f,z)=\frac{dN^{fg}/d\phi_1 d\phi_2 d\eta_1 d\eta_2 dp_{T1} dp_{T2} dN_{part} df dz}{dN^{mix}/d\phi_1 d\phi_2 d\eta_1 d\eta_2 dp_{T1} dp_{T2} dN_{part} df dz} \tag{19}$$

where both the foreground and mix distribution can be written as:

$$\begin{aligned} dN^{fg}/d\phi_1 d\phi_2... &= acc(\phi_1,\phi_2,\eta_1,\eta_2,p_{T1},p_{T2},z)\times \\ &\quad (m_0\lambda(p_{T1},p_{T2},N_{part})+g(\Delta\phi,\Delta\eta,p_{T1},p_{T2},N_{part},f)) \end{aligned} \tag{20}$$

$$dN^{mix}/d\phi_1 d\phi_2... = acc(\phi_1,\phi_2,\eta_1,\eta_2,p_{T1},p_{T2},z)m_0 \tag{21}$$

g is the jet correlation function which depends only on $\Delta\phi=\phi_2-\phi_1$,$\Delta\phi=\eta_2-\eta_1$, p_{T1},p_{T2},N_{part} and f(flavor), acc is the normalized pair acceptance function, m_0 is the background level of the underling event and λ is the ratio of the background in same event to mixed event, which is typically greater than 1. In event mixing, we treat the dependence on

[5]It is conceivable number of jets in $p-p$, n_{jet}, does not follow poisson. It is also possible that $p-p$ collision with jet also have a larger soft background associated with it, i.e, n_b and n_{jet} is not independent anymore

[6]The situation is more difficult for $Au-Au$, because in addition to jet, there is also a flow signal in same event pair distribution

z and N_{part} separately by dividing events into centrality and vertex bins[7]. In addition, we require narrow trigger and associated particle p_T bin so the p_T dependence of acc is small. In this case, Eq.20 can be rewritten as:

$$\begin{aligned} dN^{fg}/d\phi_1 d\phi_2... &= acc(\phi_1,\phi_2,\eta_1,\eta_2)(m_0\lambda + g(\Delta\phi,\Delta\eta)) \quad (22)\\ dN^{mix}/d\phi_1 d\phi_2... &= acc(\phi_1,\phi_2,\eta_1,\eta_2)m_0 \quad (23)\end{aligned}$$

the correlation function Eq.19 becomes

$$\begin{aligned} C(\phi_1,\phi_2,\eta_1,\eta_2) &= \frac{dN^{fg}/d\phi_1 d\phi_2 d\eta_1 d\eta_2}{dN^{mix}/d\phi_1 d\phi_2 d\eta_1 d\eta_2} \quad (24)\\ &= \frac{m_0\lambda + g(\Delta\phi,\Delta\eta)}{m_0}\end{aligned}$$

The typical PHENIX acceptance is shown in the Fig.2. For given trigger and associated particle p_T bin, acc is constant in that fiducial region(i.e. the trigger and partner rates are uniform.)

$$acc(\phi_1,\phi_2...) = \begin{cases} a(p_{T1},p_{T2}) & \text{for } \phi_1,\phi_2 \in [-33.75^\circ, 56.25^\circ],[123.75^\circ, 213.75^\circ], |\eta_1,\eta_2| < 0.35 \\ 0 & \text{other} \end{cases}, \quad (25)$$

Since the jet signal depends only on relative variables $\Delta\phi, \Delta\eta$, we can further simplify the CF. Lets define a set of new variables with Jacobian matrix equal to unity:

$$\begin{aligned} &\eta_1, \\ &\Delta\eta = \eta_2 - \eta_1, \\ &\phi_1, \\ &\Delta\phi = \phi_2 - \phi_1 \end{aligned} \quad (26)$$

and rewrite Eq.24 as:

$$\begin{aligned} C(\phi_1,\eta_1,\Delta\phi,\Delta\eta) &= \frac{dN^{fg}/d\phi_1, d\Delta\phi...}{dN^{mix}/d\phi_1, d\Delta\phi...} \quad (27)\\ &= \frac{acc(\phi_1,\Delta\phi..)(m_0\lambda + g)}{acc(\phi_1,\Delta\phi..)m_0} \\ &= \frac{m_0\lambda + g(\Delta\phi,\Delta\eta)}{m_0}\end{aligned}$$

Averaging Eq.27 over η_1 and ϕ_1 gives:

$$C(\Delta\phi,\Delta\eta) = \frac{1}{\Omega_{trig}}\int\int d\eta_1 d\phi_1 \frac{acc(\phi_1,\Delta\phi..)(m_0\lambda + g)}{acc(\phi_1,\Delta\phi..)m_0} = \frac{(m_0\lambda + g)}{m_0} \quad (28)$$

[7]Because we can't divide centrality accurately enough, this effectively leads to an additional normalization factor on the mix background as we shall discuss in Section.5.1

where

$$\Omega_{trig} = \int\int d\eta_1 d\phi_1 = 0.7 \times \pi \tag{29}$$

is the total trigger particle phase space.

Alternatively, we can count directly the total number of accepted pairs within given $\Delta\phi$,$\Delta\eta$, and construct a CF in a slightly different way,

$$\begin{aligned} C'(\Delta\phi,\Delta\eta) &= \frac{\int\int d\eta_1 d\phi_1 acc(\phi_1,\Delta\phi..)\,(m_0\lambda + g(\Delta\phi,\Delta\eta))}{\int\int d\eta_1 d\phi_1 acc(\phi_1,\Delta\phi..) m_0} & (30)\\ &= \frac{Acc(\Delta\phi,\Delta\eta)(m_0\lambda+g)}{Acc(\Delta\phi,\Delta\eta)m_0} & (31)\\ &= \frac{m_0\lambda+g}{m_0} \end{aligned}$$

Acc is the pair acceptance averaged over the Ω_{trig}

$$Acc(\Delta\phi,\Delta\eta,p_{T2}) = \frac{1}{\Omega_{trig}}\int\int d\eta_1 d\phi_1 acc(\phi_1,\Delta\phi,..) \tag{32}$$

One important observation is that C and C' are statistically equivalent with each other. This is true because g does not depend on η_1 and ϕ_1, so integrating CF directly(Eq.28) or integrating denominator and numerator separately(Eq.30) gives the same result.

3.2 Pair acceptance function

Understanding the acceptance function Eq.32 is crucial in obtaining the absolute normalization. Fig.5 shows the PHENIX pair acceptance in η_1,η_2 (left panel) and in $\eta_1,\Delta\eta$(middle panel). If one integrates over η_1(right panel), the resulting pair acceptance in $\Delta\eta$ is not uniform. The pair efficiency is 100% at $\Delta\eta = 0$ and decrease linearly to 0 at $|\Delta\eta| = 0.7$.

Similarly, in Fig.6 we show the the PHENIX pair acceptance in ϕ_1,ϕ_2(left top) and $\Delta\phi,\phi_1$(right top), together with the projection of the pair efficiency onto $\Delta\phi$ (middle and bottom panels). We assume both p_{T1} and p_{T2} are sufficiently large enough, such that the bending from magnetic field can be ignored [8]. The bottom panel demonstrate that with only half the azimuth coverage for single particles, PHENIX actually has sensitivity to pairs with any given $\Delta\phi$. This is the result of the special orientation of the detector in azimuth, such that the pairs accepted in the two arm covers the full azimuth. The maximum pair efficiency is 100% at $\Delta\phi = 0$, the minimum efficiency is about $0.3935/3.14159 = 12.5\%$ at $\Delta\phi = -1.57, 1.57, 4.71$. So if we have 8 times more events for these minimum efficiency region, we would get similar statistical error relative to the maximum efficiency region. The overall average pair efficiency is 50%[9].

Fig.5c and Fig.6d are just the projections of the full 2D pair acceptance function onto $\Delta\eta$ and $\Delta\phi$, respectively. There is only one point in the 2D pair acceptance function,

[8] Bending tends to make the pair acceptance more uniform.

[9] The average pair efficiency is solely determined by single particle acceptance as indicated by Fig.6.

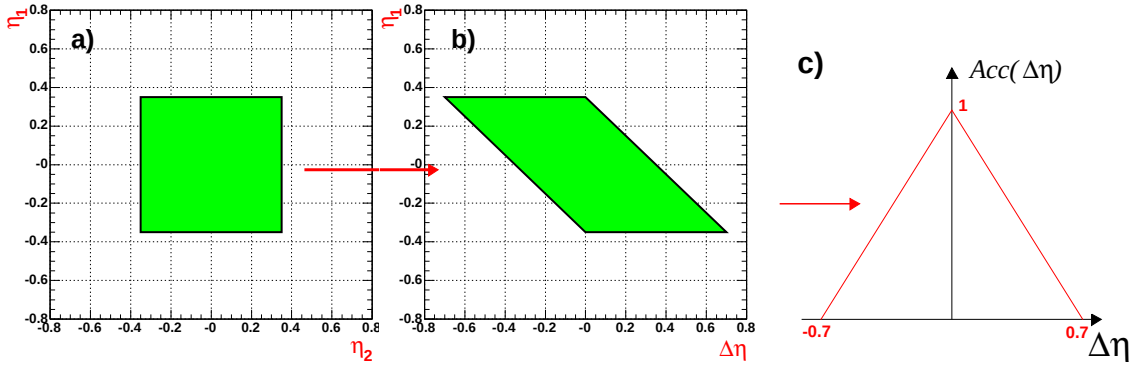

Figure 5: The PHENIX acceptance in pseudo-rapidity for particle pairs in η_1, η_2 (left panel) and in $\Delta\eta, \eta_1$(middle panel). Note that the area, which represents the total pair acceptance, is the same between the two panels. The projection on $\Delta\eta$ is shown in right panel.

$(\Delta\phi = 0, \Delta\eta = 0)$, where the pair efficiency is 100%[10]. The efficiency is below 100% at all other places. The sensitive range of the pair variables $\Delta\phi, \Delta\eta$ are significant larger than that for single particles(4 times): the acceptance in $\Delta\phi$ covers the full azimuth, $\Delta\phi \in [-0.5\pi, 1.5\pi]$ and the acceptance in $|\Delta\eta|$ is increased to $\Delta\eta < 0.7$. However, the price we have to pay is a decrease in total average pair efficiency to 25%(50% in $\Delta\phi$ and 50% in $\Delta\eta$).

The above discussion is based on the assumption that the detection efficiency for primary particles is 100% in PHENIX acceptance. However, due to decay in flight and the inefficiency of the tracking detectors, the overall detection efficiency ϵ is less than 100%. In addition, detector two track resolution and/or pair cuts in the analysis, denoted as $k\prime_{ab}(\Delta\phi, \Delta\eta)$, can further reduce pair efficiency [11]. With these factors taken into account, Eq.32 becomes

$$\begin{aligned} Acc(\Delta\phi, \Delta\eta) &= \frac{1}{\Omega_{trig}} \int\int_{acc\neq 0} d\eta_1 d\phi_1 \epsilon(\phi_1, \eta_1)\epsilon(\phi_1 + \Delta\phi, \eta_1 + \Delta\eta) \\ &\quad \times k\prime_{ab}(\Delta\phi, \Delta\eta) acc(\Delta\phi, \Delta\eta) \end{aligned} \tag{33}$$

since acc is constant with ϕ_1 and η_1, the average Acc would be the average of $\epsilon(\phi_1, \eta_1)\epsilon(\phi_2, \eta_2)$ in the PHENIX pair acceptance.

3.3 Sum rule for 2D correlation function

According to Eq.30, the measured foreground and mixed event pair distribution are,

$$\frac{dN^{mix}}{d\Delta\phi d\Delta\eta} = Acc(\Delta\phi, \Delta\eta) m_0 \tag{34}$$

$$\frac{dN^{fg}}{d\Delta\phi d\Delta\eta} = Acc(\Delta\phi, \Delta\eta)(m_0\lambda + g) \tag{35}$$

[10] Because in this case, once you accept the trigger you automatically accept the partner.
[11] This is different from the overall pair efficiency K_{ab} in Eq.10-12.

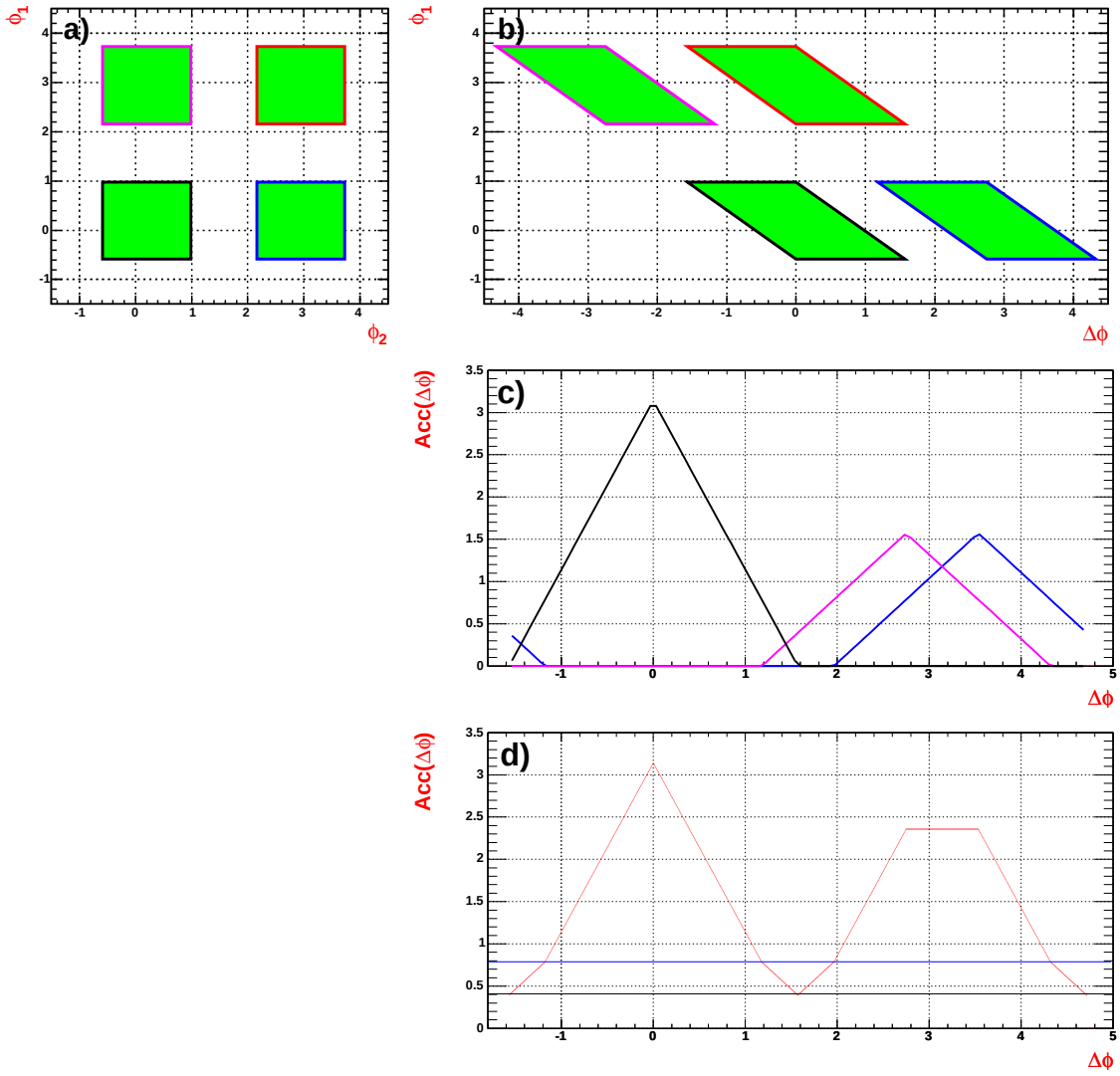

Figure 6: The PHENIX acceptance in azimuth for particle pairs in ϕ_1, ϕ_2 (top left panel) and in $\Delta\phi, \phi_1$(top right panel). Note that the area, which represents the total pair acceptance, is the same between the two panels. The projections of the patches in top right panel onto $\Delta\phi$ is shown in middle panel. The bottom panel shows the sum of all projections, thus represents the ideal pair acceptance function.

The underling rates foreground and background pairs without acceptance effect are:

$$\frac{dN_0^{fg}}{d\Delta\phi d\Delta\eta} = m_0\lambda + g(\Delta\phi, \Delta\eta) \quad (36)$$

$$\frac{dN_0^{mix}}{d\Delta\phi d\Delta\eta} = m_0 \quad (37)$$

m_0 represents the underling combinatoric background rate in the phase space covered by the pair, and should be a constant [12]. The actual number of detected pairs is just the underling background (m_0) multiplied by the pair acceptance function(Acc). Based on Fig.5 and Fig.6, this pair phase space can be summarized as,

- trigger

$$\phi_1 \in [-0.589, 0.982], [2.160, 3.731], |\eta_1| < 0.35 \tag{38}$$

  The trigger phase space is $\Omega_{trig} = \Omega_\eta \times \Omega_\phi = 0.7\pi$

- pair

$$\Delta\phi \in [-0.5\pi, 1.5\pi], |\Delta\eta| < 0.7 \tag{39}$$

  The total pair phase space is $\Omega_{pair} = \Omega_{\Delta\eta} \times \Omega_{\Delta\phi} = 2.8\pi$.

We can imagine PHENIX detector as a subset of a larger detector which have 2π acceptance in azimuth, and ± 0.7 unit rapidity coverage in η, Eq.36 and Eq.37 would correspond to the foreground and mixed background pair rates in this larger detector satisfying condition Eq.38 and Eq.39. On the other hand, the additional Acc term in Eq.34 and Eq.35 just reflects the modulation of the pair phase space shown by Fig.5c in $\Delta\eta$ and Fig.6d in $\Delta\phi$.

By integrating the correlation function, we have

$$\begin{aligned}
\int\int d\Delta\phi d\Delta\eta\, C(\Delta\phi,\Delta\eta) &= \int\int d\Delta\phi d\Delta\eta \frac{\frac{dN^{fg}}{d\Delta\phi d\Delta\eta}}{\frac{dN^{mix}}{d\Delta\phi d\Delta\eta}} \\
&= \int\int d\Delta\phi d\Delta\eta \frac{m_0\lambda + g(\Delta\phi,\Delta\eta)}{m_0} \\
&= \frac{\int\int d\Delta\phi d\Delta\eta (m_0\lambda + g(\Delta\phi,\Delta\eta))}{\frac{1}{\Omega_{pair}}\int\int d\Delta\phi d\Delta\eta m_0} \\
&= \frac{\int\int d\Delta\phi d\Delta\eta (\frac{dN_0^{fg}}{d\Delta\phi d\Delta\eta})}{\frac{1}{\Omega_{pair}}\int\int d\Delta\phi d\Delta\eta \frac{dN_0^{mix}}{d\Delta\phi d\Delta\eta}} \\
&= \frac{\langle n_{ab}\rangle^{fg}}{\frac{1}{\Omega_{pair}}\langle n_{ab}\rangle^{mix}} = \frac{\langle n_{ab}\rangle}{\frac{1}{\Omega_{pair}}\langle n_a\rangle\langle n_b\rangle}
\end{aligned} \tag{40}$$

we have used Eq.12 and setting $K_{ab} = 1$ because there is no pair cut on the underling event. $\langle n_{ab}\rangle$ is the total pairs falls in the pair acceptance given by Eq.39; $\langle n_a\rangle$ is the average number of trigger in trigger acceptance (Eq.38); $\langle n_b\rangle$ is the average partner in $|\eta| < 0.7$ and 2π in azimuth. This relation is the sum rule similar to Eq.33 in Paul's note[1].

[12]There are some non constant background correlation, examples includes resonance, global momentum conservation etc. In our current study, we assume they are small comparing to the signal.

3.4 Conditional yield for full correlation function

Along the same lines, we derive the conditional yield for PHENIX acceptance. Using from Eq.12, we rewrite the integral of the foreground distribution as:

$$\int\int d\Delta\phi d\Delta\eta \frac{dN^{mix}}{d\Delta\phi d\Delta\eta} = N_{evts} \left\langle n'_{ab} \right\rangle^{mix} = N_{evts} K'_{ab} \left\langle n'_a \right\rangle \left\langle n'_b \right\rangle \tag{41}$$

where $\langle n'_a \rangle$ is the number of type 'a' in PHENIX acceptance including detection efficiency. Similarly,

$$\int\int d\Delta\phi d\Delta\eta \frac{dN_0^{mix}}{d\Delta\phi d\Delta\eta} = N_{evts} \left\langle n_{ab} \right\rangle^{mix} = N_{evts} \left\langle n_a \right\rangle \left\langle n_b \right\rangle \tag{42}$$

there is no pair cut efficiency term ($K_{ab} = 1$) since this is the underling distribution.

From Section 3.1 we know that $\frac{dN^{fg}/d\Delta\phi d\Delta\eta}{dN^{mix}/d\Delta\phi d\Delta\eta} = \frac{dN_0^{fg}/d\Delta\phi d\Delta\eta}{dN_0^{mix}/d\Delta\phi d\Delta\eta}$, more correct form including two track resolution effect and pair cut efficiency would be

$$\frac{dN^{fg}/d\Delta\phi d\Delta\eta/k^{fg}(\Delta\phi,\Delta\eta)}{dN^{mix}/d\Delta\phi d\Delta\eta/k^{mix}(\Delta\phi,\Delta\eta)} = \frac{dN_0^{fg}/d\Delta\phi d\Delta\eta}{dN_0^{mix}/d\Delta\phi d\Delta\eta} \tag{43}$$

Combining Eq.41, Eq.42,

$$\begin{aligned} \frac{1}{N_a}\frac{dN_0^{fg}}{d\Delta\phi d\Delta\eta} &= \frac{\Omega_{pair} m_0}{N_a}\frac{dN_0^{fg}/d\Delta\phi d\Delta\eta}{\Omega_{pair} m_0} = \frac{N_{evts}\left\langle n_a \right\rangle \left\langle n_b \right\rangle}{N_a}\frac{dN_0^{fg}/d\Delta\phi d\Delta\eta}{\Omega_{pair} m_0} \\ &= \frac{N_{evts}\left\langle n_a \right\rangle \left\langle n_b \right\rangle}{\Omega_{pair} N_a}\frac{dN_0^{fg}/d\Delta\phi d\Delta\eta}{dN_0^{mix}/d\Delta\phi d\Delta\eta} \end{aligned} \tag{44}$$

where, we have multiplied the numerator and denominator a common multiplicative factor $\Omega_{pair} m_0 = \int\int d\Delta\phi d\Delta\eta \frac{dN_0^{mix}}{d\Delta\phi d\Delta\eta} = N_{evts}\left\langle n_a \right\rangle \left\langle n_b \right\rangle$. Using Eq.43, we can further simplify Eq.44:

$$\begin{aligned} \frac{1}{N_a}\frac{dN_0^{fg}}{d\Delta\phi d\Delta\eta} &= \frac{N_{evts}\left\langle n_a \right\rangle \left\langle n_b \right\rangle}{\Omega_{pair} N_a}\frac{k^{mix}(\Delta\phi,\Delta\eta) dN^{fg}/d\Delta\phi d\Delta\eta}{k^{fg}(\Delta\phi,\Delta\eta) dN^{mix}/d\Delta\phi d\Delta\eta} \\ &= \frac{\left\langle n_a \right\rangle \left\langle n_b \right\rangle}{\Omega_{pair} N_a K\prime_{ab} \left\langle n\prime_a \right\rangle \left\langle n\prime_b \right\rangle}\frac{k^{mix}(\Delta\phi,\Delta\eta) dN^{fg}/d\Delta\phi d\Delta\eta}{\frac{k^{fg}(\Delta\phi,\Delta\eta) dN^{mix}/d\Delta\phi d\Delta\eta}{\int\int d\Delta\phi d\Delta\eta dN^{mix}/d\Delta\phi d\Delta\eta}} \\ &= \frac{1}{N\prime_a}\frac{1}{K\prime_{ab}\epsilon_{asso}}\frac{k^{mix}(\Delta\phi,\Delta\eta)}{k^{fg}(\Delta\phi,\Delta\eta)}\frac{dN^{fg}/d\Delta\phi d\Delta\eta}{\frac{\Omega_{pair} dN^{mix}/d\Delta\phi d\Delta\eta}{\int\int d\Delta\phi d\Delta\eta dN^{mix}/d\Delta\phi d\Delta\eta}} \end{aligned} \tag{45}$$

Where $N\prime_a = N_{evt}\left\langle n\prime_a \right\rangle$ is the total number of triggers in PHENIX acceptance(including detection efficiency), $N_a = N_{evt}\left\langle n_a \right\rangle$ is the total number of triggers in ideal PHENIX acceptance(assume 100% efficiency), and $\epsilon_{asso} = \left\langle n\prime_b \right\rangle / \left\langle n_b \right\rangle$ is the average detection efficiency for associated particles. There is also a term $K\prime_{ab}$ that comes from the normalization of the mix distribution. $K\prime_{ab}$,k^{mix} and k^{fg} might not be 1 if one requires pair cuts on the mixed pairs. In addition, k^{fg} can deviate from 1 if the effect of detector two track resolution is large.

Eq.45 can be used to correct the measured conditional yield back to the true conditional yield. We would like to point out that the dependence on trigger particle naturally cancels out in conditional yield; however, the dependence on partner does not, in fact $\langle n\prime_b \rangle$ and $\langle n_b \rangle$ represent the average number of partners within PHENIX and the larger detector covering $|\eta| < 0.7$ and 2π in azimuth, respectively.

4 Conditional yield in 1D

In principle, one can extract the conditional yield using Eq.45; In practice, due to limited statistics, people usually study one dimensional CFs in either $\Delta\phi$ or $\Delta\eta$. In this section, we discuss the relation between 2D into 1D CFs, and we shall derive the formula that leads to the true conditional yield for 1D CFs.

4.1 Correlation function in $\Delta\phi$

In ideal PHENIX acceptance, the pair acceptance function can be factorized [13] in $\Delta\eta$ and $\Delta\phi$,

$$Acc(\Delta\phi, \Delta\eta) = Acc_1(\Delta\eta) Acc_2(\Delta\phi) \tag{46}$$

where Acc_1 and Acc_2 have the forms shown in Fig.5c and Fig.6d.

In jet signal can be written as [1],

$$g(\Delta\phi, \Delta\eta) = N_{ab}^{near} J(\Delta\phi, \sigma_1) J(\Delta\eta, \sigma_2) + N_{ab}^{far} J(\Delta\phi - \pi, \sigma_3) J(\Delta\eta, \sigma_4) \tag{47}$$

where $J(\Delta\phi, \sigma)$ is normalized gauss function with width of σ. In the near side, jet width in typically equal for $\Delta\phi$ and $\Delta\eta$. In the far side, jet correlation is broad in $\Delta\eta$.

One way to construct a 1D correlation function in $\Delta\phi$ which preserves the jet yield in Eq.45 can be written as:

$$\begin{aligned} C(\Delta\phi) &= \frac{1}{\Omega_{\Delta\eta}} \int d\Delta\eta \frac{Acc(\Delta\phi, \Delta\eta)(m_0\lambda + g(\Delta\phi, \Delta\eta))}{Acc(\Delta\phi, \Delta\eta) m_0} \\ &= \lambda + \frac{\int d\Delta\eta g(\Delta\phi, \Delta\eta)}{\Omega_{\Delta\eta} m_0} \end{aligned} \tag{48}$$

However, for technical reason, the correlation function in PHENIX is build in a slightly different way,

$$\begin{aligned} C_1(\Delta\phi) &= \frac{\int d\Delta\eta Acc(\Delta\phi, \Delta\eta)(m_0\lambda + g(\Delta\phi, \Delta\eta))}{\int d\Delta\eta Acc(\Delta\phi, \Delta\eta) m_0} \\ &= \frac{\int d\Delta\eta Acc_1(\Delta\eta)(m_0\lambda + g(\Delta\phi, \Delta\eta))}{\int d\Delta\eta Acc_1(\Delta\eta) m_0} \\ &= \lambda + \frac{I_\eta \int d\Delta\eta Acc_1(\Delta\eta) g(\Delta\phi, \Delta\eta)}{\Omega_{\Delta\eta} m_0} \end{aligned} \tag{49}$$

[13] The general condition is that the single particle efficiency function defined in Eq.33 is factorizable:$\epsilon(\phi, \eta) = \epsilon_\phi(\phi)\epsilon_\eta(\eta)$. For example, if there is a hole or low efficiency area in limited η and ϕ range, then the correlation function can not be factorized.

Where $I_\eta = \frac{\Omega_{\Delta\eta}}{\int d\Delta\eta Acc_1(\Delta\eta)}$ is the normalization factor in $\Delta\eta$. Using the functional form given by Eq.5c, we find $I_\eta = 2$ which equals to the inverse of the average pair efficiency of 50%.

C is the integral of the 2D CF, while C_1 is the ratio of the integral of the foreground pairs and mixed pairs. In general, the integration and division do not commute so they are different. C is just the average of the 2D CF in $\Delta\eta$, whereas C_1 can be treated as some kind of 'pair acceptance weighted average'. Since the pair efficiency is 100% for $\Delta\eta = 0$ and linearly decrease to 0 at $|\Delta\eta| = 0.7$, for given gauss width σ, we can calculate the ratio of the fraction of jet yields seen by the two functions,

$$R_{\Delta\eta}(\sigma) = \frac{2\int_0^{0.5\Omega_{\Delta\eta}} d\Delta\eta \frac{1}{\sqrt{2\pi}\sigma} e^{-\frac{\Delta\eta^2}{2\sigma^2}}}{2\int_0^{0.5\Omega_{\Delta\eta}} d\Delta\eta \frac{1}{\sqrt{2\pi}\sigma} e^{-\frac{\Delta\eta^2}{2\sigma^2}} \left[\frac{\Omega_{\Delta\eta}-2\Delta\eta}{\Omega_{\Delta\eta}}\right]} \tag{50}$$

The fraction of the total jet pair yield in pair acceptance (relative to their asymptotic value when jet cone is infinitely narrow) for C and C_1 and the ratio of the the fractions, $R_{\Delta\eta}$ [14], is shown in Fig.7. In this figure, $\eta_0 = 0.35$ is the maximum η for single particles. As one can see, the difference between the two is continuously changing when σ_{jet} is a few times of η_0, but when the jet width is much larger than η_0, the difference is stably at factor 2. Fig.8 is the same as Fig.7, except plotted as function of η_0, clearly one can see that even the η_0 is more than 5 times larger than jet width, the correction is still on the order of 10% level.

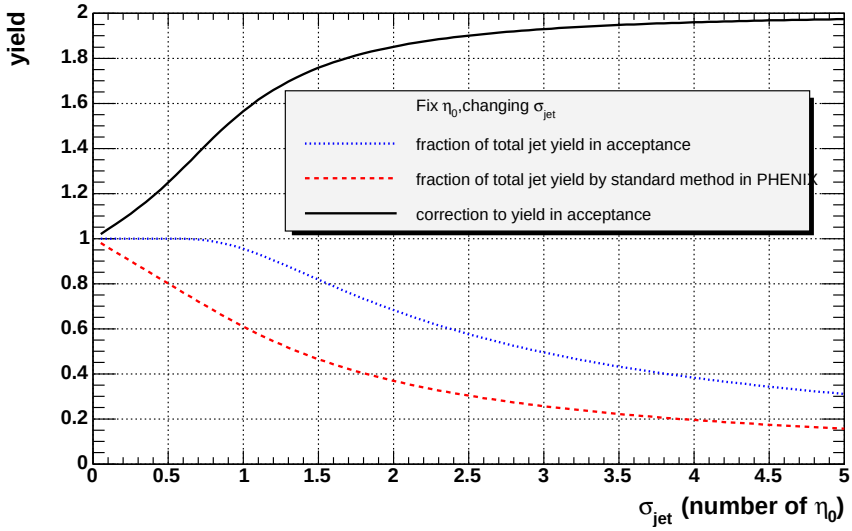

Figure 7: The fraction of underling jet(relative to the asymptotic value) yield caught by the true CF(dotted line) and the standard PHENIX CF(dashed line). And correction from dashed to dotted line. All variables are plotted as function of jet width.

We can now write down the relation between C and C_1

$$C(\Delta\phi) \;=\; \lambda + (C_1(\Delta\phi) - \lambda)\,\frac{R_{\Delta\eta}}{I_\eta} \tag{51}$$

[14] If one just make the ratio of C to C_1, there is also an additional factor I_η so the ratio of the CFs is $R_{\Delta\eta}/I_\eta$. But here we care about the fraction of total jet signal accepted.

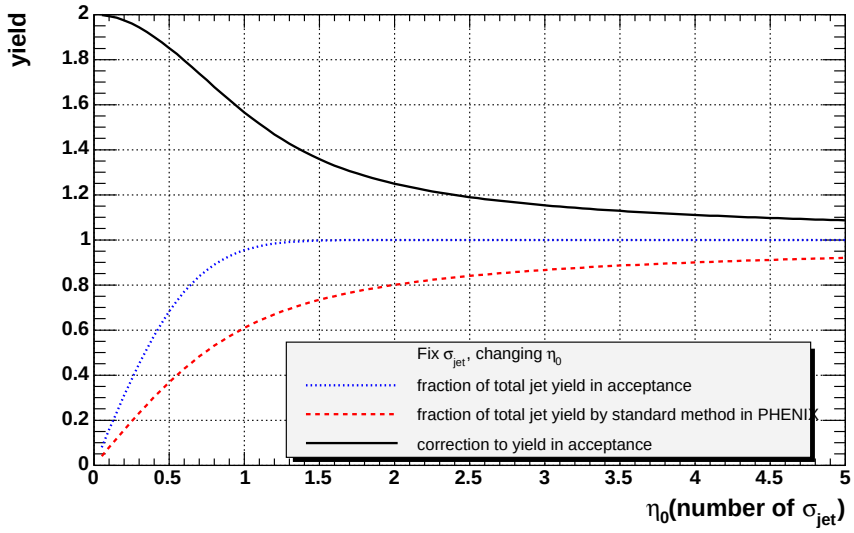

Figure 8: The fraction of underling jet yield in pair acceptance for the true CF(dotted line) and the standard PHENIX CF(dashed line). And correction from dashed to dotted line. All variables are plotted as function of PHENIX maximum pseudo-rapidity, η_0.

For $\pi^{\pm} - h$ correlation, typical jet width is 0.1-0.5 rad, the typical value of $R_{\Delta\eta} \in [1.1 - 1.8]$.

Because the fraction of near side jet yield in PHENIX pair acceptance strongly depends on the width of the jet, it makes no sense if we want to plot it against variables that depends on the jet width, like p_T of the trigger particle. The factor $R_{\Delta\eta}$ only correct the difference of fractional jet yield between C and C_1, i.e, from dashed line to dotted line in both Fig.7 and Fig.8. But there is still a fraction of jet pairs that is missed by correlation function Eq.48, which can be written as a complementary error function,

$$erfc(\frac{\sqrt{2}\eta_0}{\sigma}) = 1 - 2\int_0^{0.5\Omega_{\Delta\eta}} d\Delta\eta \frac{1}{\sqrt{2\pi}\sigma} e^{-\frac{\Delta\eta^2}{2\sigma^2}} \tag{52}$$

Thus the additional correction factor accounting for this fraction is,

$$R^1_{\Delta\eta} = \frac{1}{2\int_0^{0.5\Omega_{\Delta\eta}} d\Delta\eta \frac{1}{\sqrt{2\pi}\sigma} e^{-\frac{\Delta\eta^2}{2\sigma^2}}} \tag{53}$$

In order to correct to the full underling jet yield as given by Eq.47, we have to correct for not only the pair efficiency as shown in Eq.50 which is $R_{\Delta\eta}$, but also the fraction of the jets falls outside the pair acceptance $R^1_{\Delta\eta}$. This combined correction is:

$$\begin{aligned} R_{tot} = R_{\Delta\eta} \times R^1_{\Delta\eta} &= \frac{1}{2\int_0^{0.5\Omega_{\Delta\eta}} d\Delta\eta \frac{1}{\sqrt{2\pi}\sigma} e^{-\frac{\Delta\eta^2}{2\sigma^2}} \frac{\Omega_{\Delta\eta} - 2\Delta\eta}{\Omega_{\Delta\eta}}} \\ &\equiv \frac{1}{\int_0^{\eta_0} d\eta \left(erf\left(\frac{\eta_0 - \eta}{\sqrt{2}\sigma}\right) + erf\left(\frac{\eta_0 + \eta}{\sqrt{2}\sigma}\right)\right)} \end{aligned} \tag{54}$$

and note the denominator is the same as the one that Mickey used in his note[18].

4.2 Correlation function in $\Delta\eta$

To correct for the pair efficiency in $\Delta\eta$, one have to know the jet shape in $\Delta\eta$. When the factorization condition Eq.46 is valid, we can measure the jet shape reliably by event mixing technique. Similar to the procedure for extracting CF in $\Delta\phi$, we have,

$$\begin{aligned} C_1(\Delta\eta) &= \frac{\int d\Delta\phi Acc(\Delta\phi,\Delta\eta)(m_0\lambda + g(\Delta\phi,\Delta\eta))}{\int d\Delta\phi Acc(\Delta\phi,\Delta\eta)m_0} \\ &= \frac{\int d\Delta\phi Acc_2(\Delta\phi)(m_0\lambda + g(\Delta\phi,\Delta\eta))}{\int d\Delta\phi Acc_2(\Delta\phi)m_0} \\ &= \lambda + \frac{I_\phi \int d\Delta\phi Acc_2(\Delta\phi)g(\Delta\phi,\Delta\eta)}{\Omega_{\Delta\phi}m_0} \end{aligned} \tag{55}$$

Where $I_\phi = \frac{\Omega_{\Delta\phi}}{\int d\Delta\phi Acc_2(\Delta\phi)}$ is the normalization factor in $\Delta\phi$. Using the functional form given by Eq.6d, we find $I_\phi = 2$ which equals to the inverse of the average pair efficiency of 50%[15].

Obviously, if the jet signal follows Eq.47, then the jet width measured by above correlation function should be the correct jet width. But the yield suffers from pair efficiency loss, the missing fraction of jet pair can be evaluated straightforwardly in a way similar Eq.50, but we have to use a much more complicated pair acceptance function as shown by Fig.6d.

4.3 Sum rule and conditional yield for 1D CF

The sum rule for C follows trivially from Eq.40 and Eq.48

$$\int d\Delta\phi\ C(\Delta\phi) = \frac{\Omega_\phi \langle n_{ab}\rangle}{\langle n_a\rangle \langle n_a\rangle} \tag{56}$$

Then from the relation between C and C_1, Eq.51, we obtain the sum rule for C_1.

$$\begin{aligned} \int d\Delta\phi\ C_1(\Delta\phi) &= \frac{I_\eta}{R_{\Delta\eta}} \int d\Delta\phi C(\Delta\phi) - \left[\frac{I_\eta}{R_{\Delta\eta}} - 1\right] \lambda\Omega_{\Delta\phi} \\ &= \frac{I_\eta\Omega_\phi}{R_{\Delta\eta}} \frac{\langle n_{ab}\rangle}{k_{ab}\langle n_a\rangle\langle n_a\rangle} - \left[\frac{I_\eta}{R_{\Delta\eta}} - 1\right] \lambda\Omega_{\Delta\phi} \end{aligned} \tag{57}$$

Since the overall pair acceptance are different for mixed pair and jet pairs in η, it is not surprising that we get an additional term in Eq.57 for C_1.

Eq.41 and Eq.42 become,

$$\int d\Delta\phi \frac{dN^{mix}}{d\Delta\phi} = N_{evts}\langle n'_{ab}\rangle^{mix} = N_{evts}K'_{ab}\langle n'_a\rangle\langle n'_b\rangle \tag{58}$$

$$\int d\Delta\phi \frac{dN_0^{mix}}{d\Delta\phi} = N_{evts}\langle n_{ab}\rangle^{mix} = N_{evts}\langle n_a\rangle\langle n_b\rangle \tag{59}$$

[15] I_ϕ is equal to I_η, this is an accident because the fact that the PHENIX acceptance in ϕ is half of the full azimuth.

In general, the relation Eq.41 for 2D correlation is not valid for the 1D correlation, i.e. $\frac{dN^{fg}/d\Delta\phi}{dN^{mix}/d\Delta\phi} \neq \frac{dN_0^{fg}/d\Delta\phi}{dN_0^{mix}/d\Delta\phi}$, instead,

$$\frac{dN^{fg}/d\Delta\phi - \lambda dN^{mix}/d\Delta\phi}{dN^{mix}/d\Delta\phi} = \frac{I_\eta}{R_{\Delta\eta}}\left(\frac{dN_0^{fg}/d\Delta\phi - \lambda dN_0^{mix}/d\Delta\phi}{dN_0^{mix}/d\Delta\phi}\right) \tag{60}$$

This relation is easy to understand. Basically, the numerator and the denominator in the LHS represents the measured jet pairs and mix background pairs, respectively, and similarly observation can be make about RHS. The relation between the measured mix background and underling background we choose is,

$$dN_0^{mix}/d\Delta\phi \propto I_\eta dN^{mix}/d\Delta\phi \tag{61}$$

where the I_η just accounts for the pair efficiency of the mixed background in η. The relation between the detected jet signal and the underling jet signal is

$$dN_0^{fg}/d\Delta\phi - \lambda dN_0^{mix}/d\Delta\phi \propto R_{\Delta\eta}(dN^{fg}/d\Delta\phi - \lambda dN^{mix}/d\Delta\phi) \tag{62}$$

$R_{\Delta\eta}$ accounts for the correction of the jet yield in $|\Delta\eta| < 0.7$. The JET conditional yield follows[16],

$$\begin{aligned}
\frac{1}{N_a}\left(\frac{dN_0^{fg}}{d\Delta\phi} - \lambda\frac{dN_0^{mix}}{d\Delta\phi}\right) &= \frac{\Omega_{\Delta\eta}m_0}{N_a}\left(\frac{dN_0^{fg}/d\Delta\phi}{\Omega_{\Delta\eta}m_0} - \lambda\right) &(63)\\
&= \frac{N_{evts}\langle n_a\rangle\langle n_b\rangle}{\Omega_{\Delta\phi}N_a}\left(\frac{dN_0^{fg}/d\Delta\phi}{dN_0^{mix}/d\Delta\phi} - \lambda\right)\\
&= \frac{N_{evts}\langle n_a\rangle\langle n_b\rangle}{\Omega_{\Delta\phi}N_a}\frac{R_{\Delta\eta}}{I_\eta}\left(\frac{dN^{fg}/d\Delta\phi}{dN^{mix}/d\Delta\phi} - \lambda\right)\\
&= \frac{R_{\Delta\eta}}{I_\eta}\frac{1}{K\prime_{ab}}\frac{1}{N\prime_a\epsilon_{asso}}\frac{dN^{fg}/d\Delta\phi - \lambda dN^{mix}/d\Delta\phi}{\frac{\Omega_{\Delta\phi}dN^{mix}/d\Delta\phi}{\int d\Delta\phi dN^{mix}/d\Delta\phi}} &(64)
\end{aligned}$$

Note the difference between Eq.45 and Eq.64, the later have background contribution subtracted. This is because the combinatoric background for 1D CF do not follow the same sum rule as the signal but they do for 2D CF. We can compare Eq.64 with Mike's conditional yield formula Eq.8 in [17]. They only differ by an additional correction factor$R_{\Delta\eta}$.

We can simplify Eq.64 a little bit by absorbing all correction factors into ϵ_{asso},

$$\frac{1}{N_a}\left(\frac{dN_0^{fg}}{d\Delta\phi} - \lambda\frac{dN_0^{mix}}{d\Delta\phi}\right) = \frac{1}{N\prime_a\epsilon_{asso}}\frac{dN^{fg}/d\Delta\phi - \lambda dN^{mix}/d\Delta\phi}{\frac{\Omega_{\Delta\phi}dN^{mix}/d\Delta\phi}{\int d\Delta\phi dN^{mix}/d\Delta\phi}} \tag{65}$$

where

$$\epsilon_{asso} = \frac{I_\eta K\prime_{ab}}{R_{\Delta\eta}}\frac{\langle n\prime_b\rangle}{\langle n_b\rangle} \tag{66}$$

[16]Note here, we only looks at the conditional yield of the signal

again,$I_\eta = \frac{\Omega_{\Delta\eta}}{\int d\Delta\eta Acc_1(\Delta\eta)} = 2$ is the normalization factor in $\Delta\eta$, $\langle n_b \rangle = \Omega_{\Delta\eta}\Omega_{\Delta\phi}\frac{dN^2}{dp_T d\phi d\eta}$ is the total number of generated associated particles in phase space $\Omega_{\Delta\eta}\Omega_{\Delta\phi}$.

So far, we have ignored the pair cut efficiency exist in the foreground pair distribution and mix pair distribution in the 2D CF Eq.45. To include them, we have to calculate the weighted averages of the pair cut efficiency as,

$$\begin{aligned} \frac{1}{k^{fg}(\Delta\phi)} &= \frac{\int d\Delta\eta \frac{1}{k^{fg}(\Delta\phi,\Delta\eta)}\frac{dN^{fg}}{d\Delta\phi d\Delta\eta}}{\int d\Delta\eta \frac{dN^{fg}}{d\Delta\phi d\Delta\eta}} \\ \frac{1}{k^{mix}(\Delta\phi)} &= \frac{\int d\Delta\eta \frac{1}{k^{mix}(\Delta\phi,\Delta\eta)}\frac{dN^{mix}}{d\Delta\phi d\Delta\eta}}{\int d\Delta\eta \frac{dN^{mix}}{d\Delta\phi d\Delta\eta}} \end{aligned} \tag{67}$$

which leads to the most general form of the pair efficiency,

$$\epsilon_{asso} = \frac{I_\eta K\prime_{ab}}{R_{\Delta\eta}}\frac{k^{fg}(\Delta\phi)}{k^{mix}(\Delta\phi)}\frac{\langle n\prime_b\rangle}{\langle n_b\rangle} \tag{68}$$

In general, $k^{mix}(\Delta\phi,\Delta\eta)$ and $k^{fg}(\Delta\phi,\Delta\eta)$ are not equal because the two track resolution only affects the k^{fg}. But even if they are identical, since $dN^{fg}/d\Delta\phi d\Delta\eta$ and $dN^{mix}/d\Delta\phi d\Delta\eta$ have different shape, the weighted average is not equal, $k^{mix}(\Delta\phi) \neq k^{fg}(\Delta\phi)$.

Note that $\langle n'_b\rangle$ is the total number of detected associated particles, so $\frac{\langle n'_b\rangle}{\langle n_b\rangle}$ represents the average efficiency of detecting associated particles, which we can be rather accurately approximated by the single particle efficiency in PHENIX.

$$\frac{\langle n'_b\rangle}{\langle n_b\rangle} = \frac{\left(\frac{dN}{dp_T}\right)^{raw}}{\Omega_{\Delta\eta}\frac{d^2N}{dp_T d\eta}} = \frac{\epsilon_{single}}{\Omega_{\Delta\eta}} \tag{69}$$

where ϵ_{single} represents the single particle efficiency for 2π azimuth and ONE unit pseudo-rapidity!!. As we shall discuss in Section.5, our final formula is equivalent to the one Anne use in her analysis [16].

So finally the reduced efficiency correction takes the following form

$$\epsilon_{asso} = \frac{I_\eta K\prime_{ab}\epsilon_{single}}{R_{\Delta\eta}\Omega_{\Delta\eta}}\frac{k^{fg}(\Delta\phi)}{k^{mix}(\Delta\phi)} = \frac{2K\prime_{ab}\epsilon_{single}}{R_{\Delta\eta}\Omega_{\Delta\eta}}\frac{k^{fg}(\Delta\phi)}{k^{mix}(\Delta\phi)} \tag{70}$$

Similarly, we can write down also the final 2D correlation function and the corresponding efficiency as:

$$\frac{1}{N_a}\frac{dN_0^{fg}}{d\Delta\phi d\Delta\eta} = \frac{1}{N\prime_a}\frac{1}{\epsilon_{asso}}\frac{dN^{fg}/d\Delta\phi d\Delta\eta}{\frac{\Omega_{pair}dN^{mix}/d\Delta\phi d\Delta\eta}{\int\int d\Delta\phi d\Delta\eta dN^{mix}/d\Delta\phi d\Delta\eta}} \tag{71}$$

$$\epsilon_{asso}\left(\Delta\phi,\Delta\eta\right) = \frac{K\prime_{ab}\epsilon_{single}\left(\Delta\phi,\Delta\eta\right)}{\Omega_{\Delta\eta}}\frac{k^{fg}\left(\Delta\phi,\Delta\eta\right)}{k^{mix}\left(\Delta\phi,\Delta\eta\right)} \tag{72}$$

Using Paul Stankus notation [1], Eq.65 can be rewritten as,

$$\begin{aligned}\frac{1}{N_a}(\frac{dN_0^f}{d\Delta\phi}-\xi\frac{dN_0^{mix}}{d\Delta\phi}) &= \frac{1}{N_a}\left[N_{ab}^{Jet,near}J_{near}(\Delta\phi)+N_{ab}^{Jet,far}J_{far}(\Delta\phi)\right] \\ &= \left[\frac{\left\langle n_{ab}^{Jet,near}\right\rangle}{\langle n_a\rangle}J_{near}(\Delta\phi)+\frac{\left\langle n_{ab}^{Jet,far}\right\rangle}{\langle n_a\rangle}J_{far}(\Delta\phi)\right]\end{aligned} \tag{73}$$

In summary, the procedure we use to extract the conditional yield is to normalize the correlation function according to Eq.65 and then fit to Eq.73 to extract the raw conditional yield. We then have to apply the efficiency Eq.70 to obtain the true conditional yield.

5 Discussions

5.1 The foreground pedestal λ.

As we mentioned in Section.2.4, the background rate in same pair distribution can be larger than pair rates from event mixing, i.e the pedestal factor, λ, calculated as the ratio of the two is larger than 1. Several factors can contribute to λ. Most noticeably the residual multiplicity fluctuation, ξ, and additional fluctuation associated with jet production μ. We can rewrite λ as,

$$\lambda = \xi\mu. \tag{74}$$

In deriving Eq.40 and Eq.45, we have assumed that type 'a' and type 'b' are not correlated with each other(purely combinatoric). However, we have to take into account the residual multiplicity fluctuations arising from the resolution on the centrality determination (in the case of $d-Au$). This residual multiplicity leads to a intrinsic correlation between n_a and n_b, thus the true number of combinatoric pairs is larger, i.e, if we define ξ as,

$$\xi = \frac{\langle n_{ab}\rangle^{mix}}{K_{ab}\langle n_a\rangle\langle n_b\rangle} \tag{75}$$

then $\xi > 1$.

Paul stankus's have derived a general formula [1] for ξ (Eq.16). If we assume the multiplicity being proportional to the number of collisions, and the particle production is independent for each collisions. Then

$$\xi = 1+\left(\frac{\sigma(N_{coll})}{\bar{N_{coll}}}\right)^2 \tag{76}$$

independent of the probability distribution for individual collisions. In [17], ξ has been evaluated for assuming particle production is proportional to either N_{coll} or N_{part} dependence. And the final value is typically between 1 to 2.

In Section.2.4, we have discussed the additional fluctuation associated with jets and have argued that the increase of λ as function of $p_{T,asso}$ is mostly due to the multi-jet production. We denote this effect with μ.

As example (can also demonstrate with pythia) Fig.9a shows the pedestal factor λ evaluated from $\pi^{\pm} - h$ correlation for different centralities in $d - Au$ and $p - p$. There are two features to this figure: 1) an increase of λ from $p - p$ to central $d - Au$ collisions, 2) an increase of λ as function of $p_{T,asso}$. Fig.9b shows the ratios of the λ for three $d - Au$ centralities and $p - p$ to that for $d - Au$ minimum bias collisions, the p_T dependence almost cancelled out, and the λ can be factorized into a centrality dependent part, which corresponds to ξ, and a p_T dependent part, which corresponds more or less to μ.

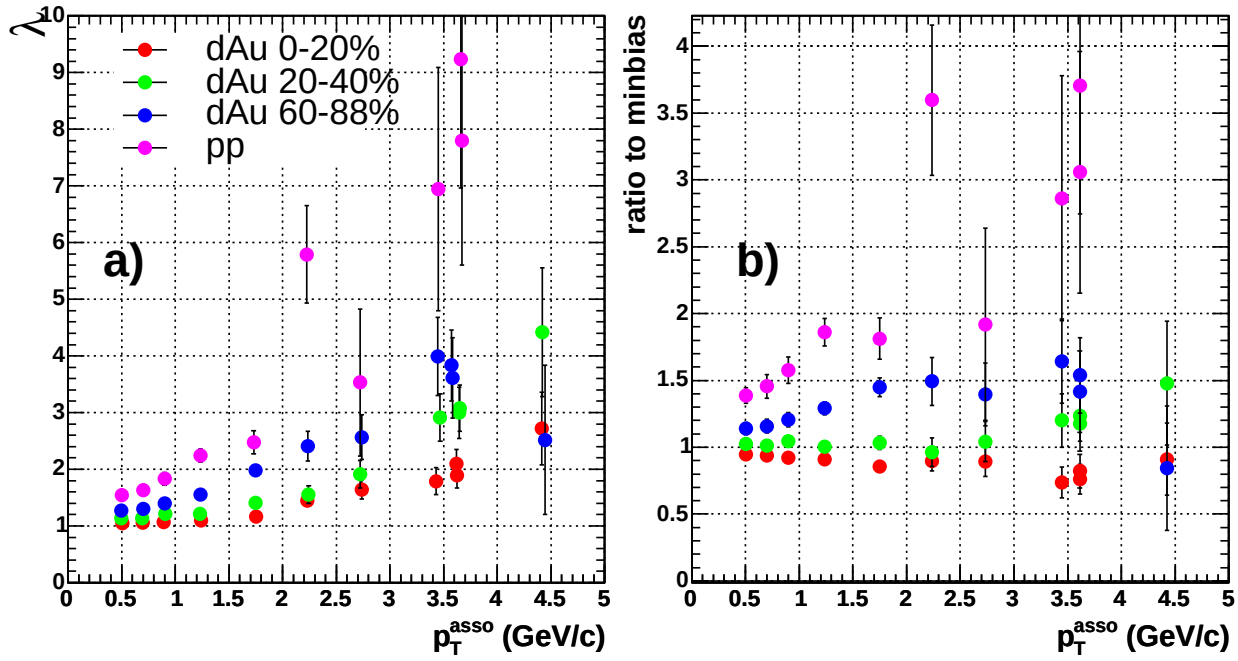

Figure 9: Left panel shows the pedestal factor λ as function of associated particle p_T for $p - p$ and 3 $d - Au$ centrality classes. Right panel shows the ratio of λ for these 4 classes to that for $d - Au$ minimum bias.

5.2 Check the formula with simple simulation

The validity of our formula can be checked with simple simulation. In the simulation, we generate both the trigger and associated particles according to the discussion on various background contributions in Section.2.4. The trigger p_T is fixed at 7 GeV/c, while the associated particle p_T is fixed for a given event, but vary from event to event. The list of possible p_Ts for the associated particles are : 0.5, 0.7, 0.9, 1.3, 1.8, 2.3, 2.8 and 4 GeV/c. We generate three different sources of particles that we generated,

1. Trigger particle arising soft background
   The number of triggers follows poisson statistics with a mean of $\langle n_a \rangle = 0.01$. Triggers were generated uniformly in $|\eta| < 0.35$ and full azimuth.

2. Associated particle arising from soft background

The number of triggers follows poisson statistics with a mean of $\langle n_b \rangle = 2$. Associated particles were generated uniformly in $|\eta| < 2$ and full azimuth.

3. Trigger and associated particle arising from jet fragmentation
The number of jets follows poisson statistics with a mean of $\langle n_{jet} \rangle = 0.2$. Each jet is fragmented to one trigger and one associated particle, with $\left\langle \vec{j_T} \right\rangle = 0.6$ GeV/c. The associated particle is generated in a way such that it's angle with the jet direction should be strictly gauss in both η and ϕ.

We generates about one million events for each of the eight associated particle p_T. Then we run the same analysis code we used for the real data analysis to make the same event pairs and mixed-event pairs, where each trigger particle from every event are mixed with the associated particles from a randomly selected event. Top panel of Fig.10 shows the typical same event pair $\Delta\eta$ distribution decomposed into the five different contributions as listed in Section2.4. The except the one labelled as '$jet_{trig} - jet_{asso}$(same jet)', all other four types pairs are backgrounds, which actually is described by mixed event distribution shown in the bottom panel. The main backgrounds are basically flat in $|\Delta\eta| < 2$, except '$soft_{trig} - jet_{asso}$' and $jet_{trig} - jet_{asso}$(different jet)' type of pairs, this is because the fact that we have required that the trigger falls within $|eta| < 0.35$. As comparison, Fig.11 shows the pair $\Delta\phi$ distribution for the five type of backgrounds with the same legend.

After making the pairs, we attempt to extract the CF and the conditional yield using the formula described in previous chapter. Since we generate only one trigger and one associated particles, the input conditional yield is expected to be 1. We extract the conditional yield for two cases: with and without the requirement that the trigger and associated particles are within the PHENIX acceptance(note that the trigger was generated with in PHENIX η acceptance already). In the later case, since we don't have any constraint on the associated particle, the raw condition yield obtained according to Eq.65 should be the true conditional yield without any further correction (because $\epsilon_{asso} = 1$). In the former case, we still need to correct the raw condition yield by ϵ_{asso} as defined by Eq.70. As an example to illustrate the procedure in obtaining the raw conditional yield, Fig.12 shows $\Delta\phi$ correlation for associated particle $p_T = 0.5$ GeV/c. The correlation in $\Delta\phi$ without requiring particles to be within PHENIX acceptance(top 3 panels) and requiring both particles to be within PHENIX acceptance (bottom 3 panels) for associated $p_T = 0.5$ GeV/c. The left panel shows the foreground pair distribution(black) and mixed pair distribution(blue). We did the simultaneous fit on the foreground and background to obtain the gauss shape, the fit range is from -1.57 to 1.57 in $\Delta\phi$ [17]. The middle panel shows the CF function as defined by Eq.49, together with the fit properly scaled from the left panel. In the right panel, we show the conditional yield[18], together with the fitted value of the yield given by the second fit parameter, p_1. In current simulation, we didn't model the seagull effect on the j_T, which will leads to a much narrower correlation width than the one shown in Fig.12. The typically extracted j_T in $\pi^{\pm} - h$ correlation for $p_{T,asso} = 0.5$ is about $\left\langle \vec{j_T} \right\rangle = 0.25$ GeV/c more than factor of two smaller than

[17] Clearly since the associated particle p_T is so small, if we would also model the away side jet, there should be a significant contamination from of the gaussian tail the away side peak. This is interesting in its own right, however a detail study is beyond the scope of current framework.

[18] it almost Eq.65, except that the background was not subtracted yet.

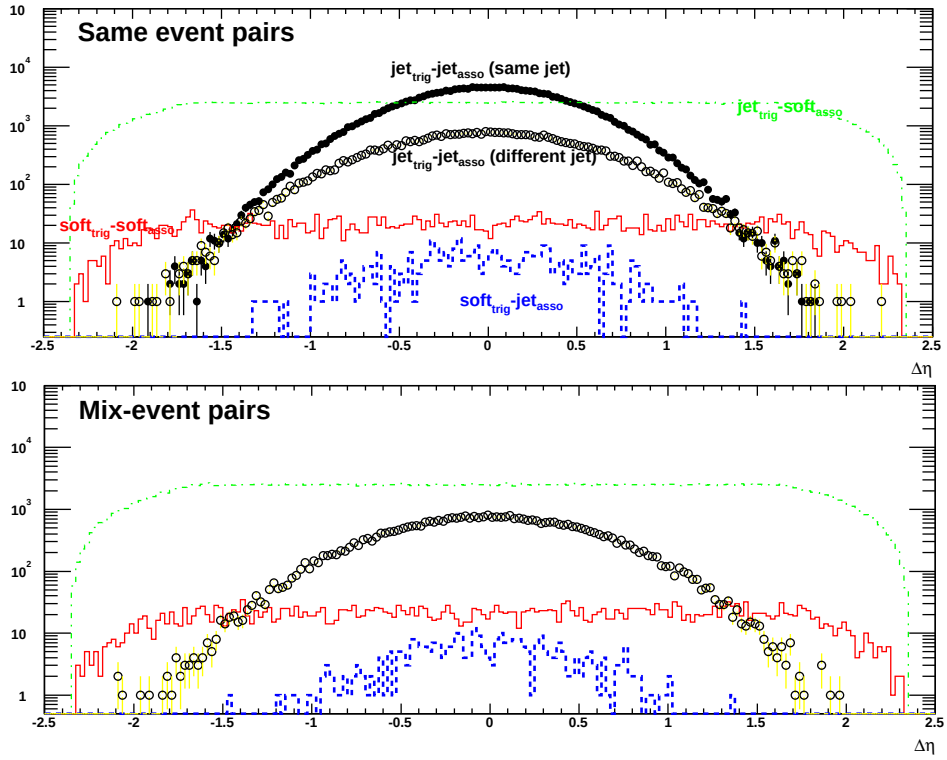

Figure 10: The decomposition of different sources of pairs contribution in the same event pair distribution(top panel) and mixed pair distribution (bottom panel). There are five different sources of pairs in the same event pairs, 1) soft trigger with soft associated particles(solid line), 2) soft trigger with associate particles from jet(dashed line), 3) trigger from jet with soft associated particles(dot dashed line), 4) trigger and associated particles from different jets (open circles), and 5) trigger and associated particles from the same jet (solid circles). There are four different sources of pairs in the mixed event pairs (same legend as foreground).

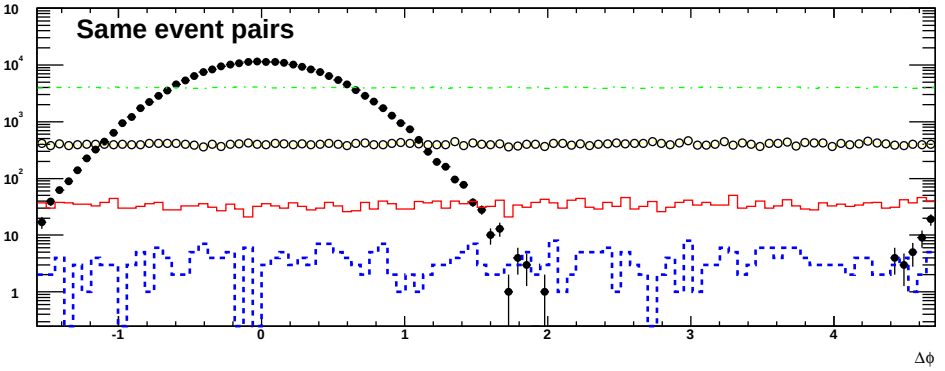

Figure 11: The decomposition of different sources of pairs contribution in the same event pair distribution. The five different sources of pairs have the same legend as the top panel of Fig.10.

the value we are using right now (0.6 GeV/c).

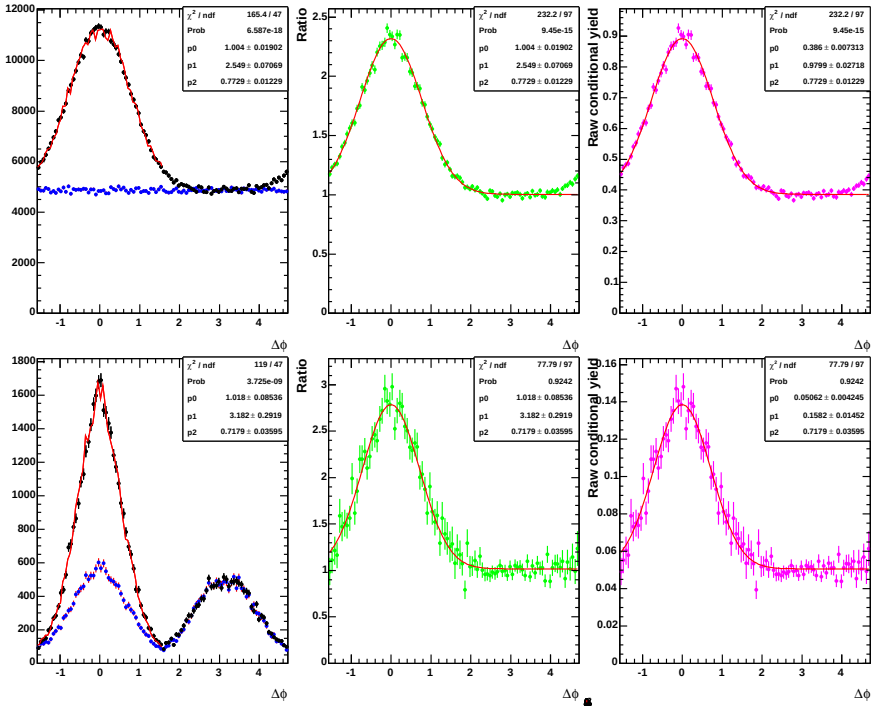

Figure 12: The correlation in $\Delta\phi$ without requiring particles to be within PHENIX acceptance(top 3 panels) and requiring both particles to be within PHENIX acceptance (bottom 3 panels) for associated $p_T = 0.5$ GeV/c. The left panel shows the foreground pair distribution(black) and mixed pair distribution(blue). We did the simultaneous fit on the foreground and background to obtain the gauss shape, the fit range is from -1.57 to 1.57 in $\Delta\phi$. The middle panel shows the CF function as defined by Eq.49, together with the fit properly scaled from the left panel. In the right panel, we show the conditional yield, together with the fitted value of the yield given by the second fit parameter, p_1.

We repeat the same procedure for each of the associated p_T, build the CF, extract the raw conditional yield from the fit then do the efficiency correction. Fig.13 shows the fitted λ value(left panel), the final conditional yield(middle panel), and the correction ϵ_{asso}(right panel), all plotted as function of jet width(0.5 GeV/c for the most right point and 4 GeV/c for the most left point). The open circle represents extracted values without imposing the PHENIX acceptance on trigger and associated particles, while the close circle represents those with the PHENIX acceptance requirement. Note that the correction on the right panel is for the one with the acceptance cuts. The line in the left and middle panel is the expectation values. Since we didn't put in any sort of multiplicity smearing the pedestal λ obtained is actually very close to 1. In all, we see that with the full correction, the condition yield very well reproduced by our procedure.

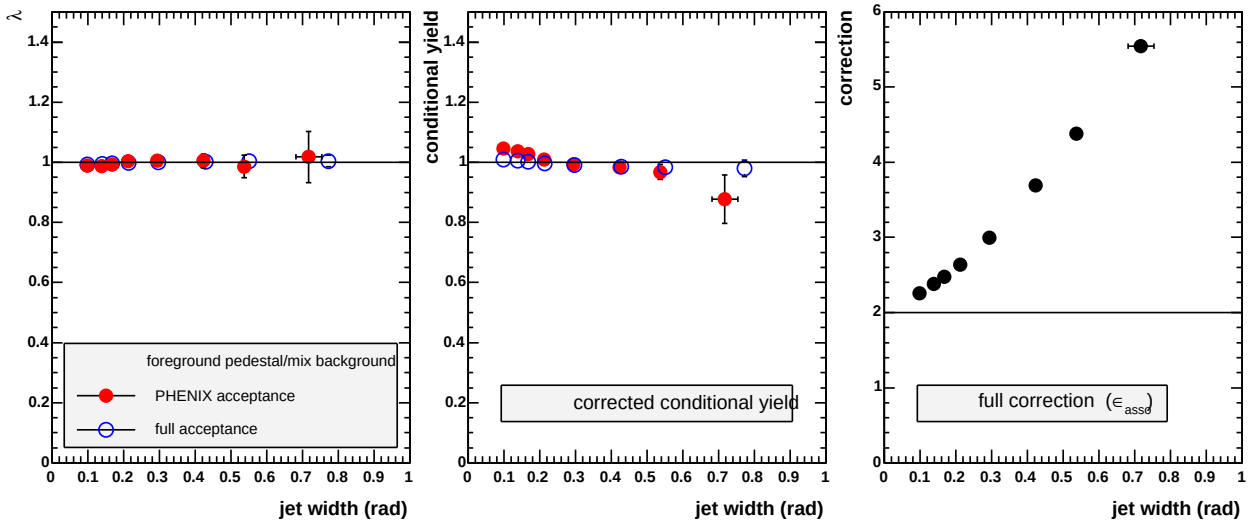

Figure 13: Shown are the fitted λ value(left panel), the final conditional yield(middle panel), and the correction ϵ_{asso}(right panel), all plotted as function of jet width(0.5 GeV/c for the most right point and 4 GeV/c for the most left point). The open circle represents extracted values without imposing the PHENIX acceptance on trigger and associated particles, while the close circle represents those with the PHENIX acceptance requirement. Note that the correction on the right panel is for the one with the acceptance cuts. The line in the left and middle panel is the expectation values.

5.3 Check the formula with pythia simulation

One of the assumption in our formula is that the combinatoric background level m_0 should not depends on $\Delta\eta$ (Eq.37). Clearly, this assumption will break down for large η value because the single particle distribution in η starts to fall around 0.5 as shown in Fig.14a. This distribution was plotted for all particles with $p_T > 1.5$GeV/c, the width is larger for lower p_T cut. One can see that even for a relative small eta window ,$|\eta| < 0.5$, the non-flatness is noticeable(about 10%). This non-flatness usually propagate into the pair $\Delta\eta$ distribution. In Fig.14b, we plot combinator pair distribution in $\Delta\eta$ requiring fixed η window on one particle($|\eta_1| < 0.35$), and varying η window on the other particle: blue $|\eta_2| < 0.35$, green $|\eta_2| < 0.5$ and red $|\eta_2| < 1$, black no cut. The pair distribution corresponding to no cut on second particles is not flat, event with narrower cut on the $|\eta_2| < 1$, the shape of the pair distribution is not triangle or trapezoidal [19] anymore. When we require both particles to be within PHENIX η acceptance, $|\eta_1| < 0.35$ and $|\eta_2| < 0.35$, the resulting pair distribution(blue) spans from -0.7 to 0.7. In this range, the true underling pair distribution actually drop by 20% from η=0 to $|\eta| = 0.7$. This is not a problem when the jet cone is narrow, but would leads to some additional correction for wider jet and should always affect the wayside jet. In fact, since we divide the foreground pair distribution by the mixed pair distribution, some of the variations in the away side jet shape in η cancelled out.

[19]The pair distribution has a trapezoidal shape if one require different η ranges for the trigger and associated particles.

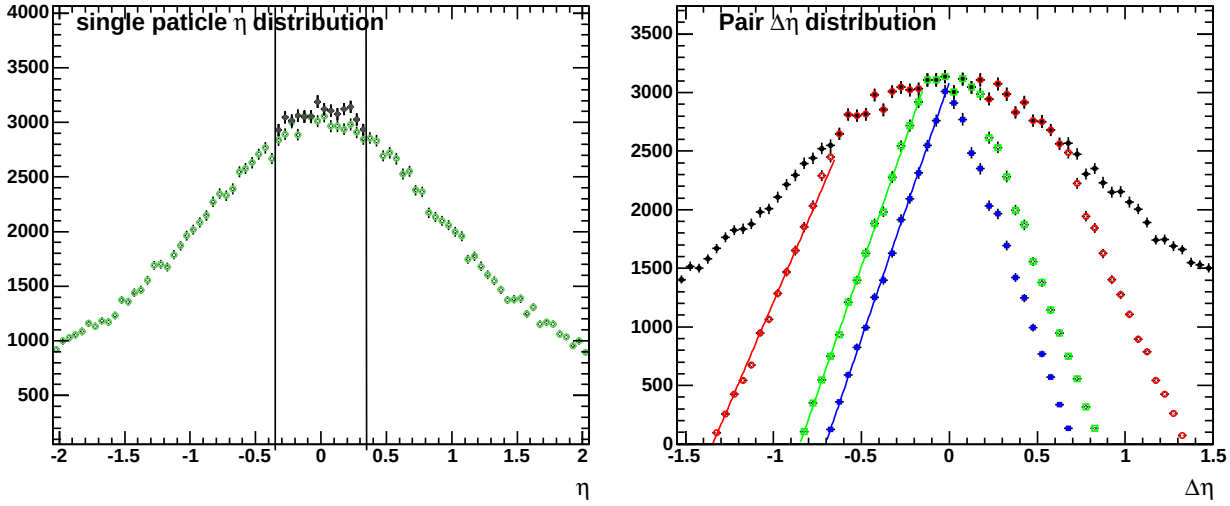

Figure 14: Left panel shows single particle pseudo-rapidity distribution for trigger with $p_T > 6$ GeV/c(black) and associated particle $p_T > 1.5$ GeV/c(light green). The trigger is required to be within PHENIX acceptance $|\eta| < 0.35$. Right panel shows the pair $\Delta\eta$ distribution for fixed trigger cut of $|\eta_1| < 0.35$ and different associated particle cut: blue $|\eta_2| < 0.35$, green $|\eta_2| < 0.5$ and red $|\eta_2| < 1$, black no cut.

Based on these considerations, we repeat the conditional yield analysis using pythia events. Two classes of pythia events, one million events each, are generated. In each event of the first class, we enable hard-scattering with minimum p_T of 10 GeV/c. Events in the second class have hard-scattering enable but no p_T cut off. We use the first class as triggered event sample, and the second class as minimum bias event sample. The same event mixing procedures used in real data analysis were repeated, where the trigger particle from the triggered events are mixed with the associated particles in the minimum bias events. The trigger particles are required to have $p_T > 6$ GeV/c, and associated particle are required to be one of the following eight cases: $0.4 < p_T < 0.6$, $0.6 < p_T < 0.8$, $0.8 < p_T < 1.0$,$1.0 < p_T < 1.5$,$1.5 < p_T < 2.0$,$2.0 < p_T < 2.5$,$2.5 < p_T < 3.0$ $3.0 < p_T < 4.0$ GeV/c. Also, in order to cross check the conditional yield extract for same side jet and away side jet, we repeat the analysis for three types of acceptance requirement.

1. Type a: Trigger particle $|\eta_{trig}| < 0.35$, no cut on associated particle, no pair cuts.

2. Type b: Trigger particle $|\eta_{trig}| < 0.35$, pair cut $|\Delta\eta| < 0.7$, i.e we requires the associated particle is ± 0.7 unit pseudo-rapidity around the trigger.

3. Type c: Both trigger and particle in PHENIX acceptance.

On the same side, the Type a should give the true conditional yield. If the correction we apply for Type c is correct, the extracted conditional yield should match that for Type a. On the far side, since PHENIX acceptance (Type c) can only detect the jet pairs in the range of $|\Delta\eta| < 0.7$, we attempt to correct the conditional yield to $|\Delta\eta| < 0.7$. So by comparing

the corrected yield with the yield obtained from Type b, we can find out how much error in the away side jet yield.

Fig.15 shows three sets of histograms corresponding to Type a(top row), Type b(middle row), and Type c(bottom row). The associated particle $1 < p_T < 1.5$ GeV/c. For each type, the left panel shows the foreground (black histogram) and mixed background (blue histogram) together with the simultaneous fit of the two histogram to a double gauss function, i.e, we assume,

$$fg(\Delta\phi) = \left(\lambda + \frac{Y_1}{\sqrt{2\pi}\sigma_1} e^{-\frac{\Delta\phi^2}{2\sigma_1^2}} + \frac{Y_2}{\sqrt{2\pi}\sigma_2} e^{-\frac{(\Delta\phi-\pi)^2}{2\sigma_2^2}} \right) \times bg(\Delta\phi) \tag{77}$$

The middle panel shows the CF Eq.49 together with the fit determined in the left panel, one notice that the same side and away side does not fits well with a gauss, presumably, this is due to the radiation process that enhance the tail of the gauss [20]. The right panel shows the raw conditional yield distribution(note that the background hasn't been subtracted). The fitted parameter p_1 for Type a(top right panel) would corresponds to the full same side jet yield, where $p_1^a = 0.7175$. The p_2 in the for Type b (middle right panel), $p_2^b = 0.9249$ would correspond to the away side jet conditional yield in $|\Delta\phi| < 0.7$. The p_1^c and p_2^c for Type c (bottom right panel), where $p_1^c = 0.2793$ and $p_2^c = 0.2331$, corresponds to the conditional yield for same side and away side in PHENIX acceptance, respectively. We then correct p_1^c and p_2^c according to Eq.70, if this correction is right, and also the rapidity dependence of single particle multiplicity is small in $|\Delta\eta| < 0.7$, then we expect that the corrected value should be equal to p_1^a and p_2^b respectively.

In Fig.16, we show the final corrected yield as function of $p_{T,asso}$ for the near side jet(left panel) and far side jet(middle panel). The expected conditional yield (solid circle) and the fully corrected conditional yield (open circle) are shown for both cases. In the left panel, for completeness, we also shows the pedestal level λ, clearly, we sees a very similar increase of the pedestal factor as function $p_{T,asso}$ as the real data discussed in Section.2.4. To check the difference between the expected conditional yield and fully corrected conditional yield, we make the ratio of the two and plot in Fig.17 for the near side jet (left panel) and far side jet (right panel). The difference is less than 10%, this demonstrate that our procedure of conditional yield extraction is correct!

[20]However, statistically, one should still get the correct yield, the fit tends to undershoot the peak but overshoot the tail.

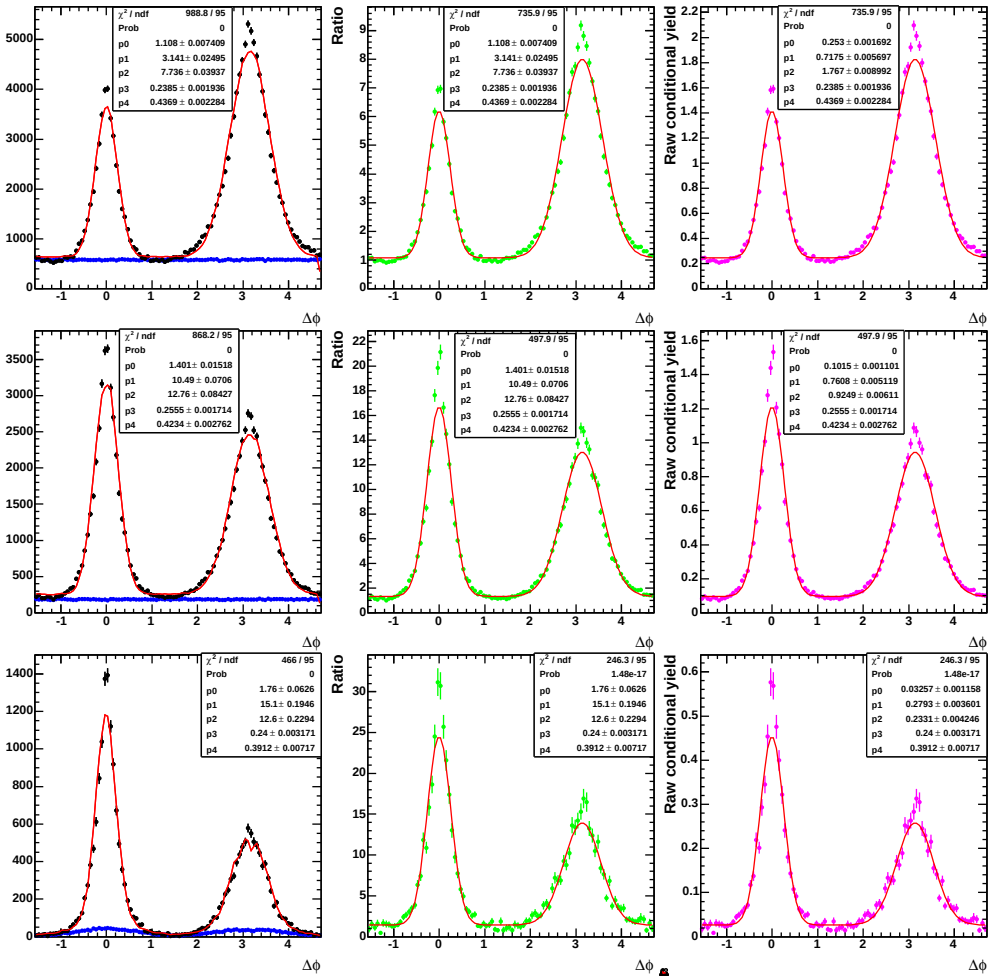

Figure 15: The figure shows three sets of histograms corresponding to Type a(top row), Type b(middle row), and Type c(bottom row). The associated particle $1 < p_T < 1.5$ GeV/c. For each type, the left panel shows the foreground (black histogram) and mixed background (blue histogram) together with the simultaneous fit of the two histogram to a double gauss function; The middle panel shows the CF Eq.49 together with the fit determined in the left panel; The right panel shows the raw conditional yield distribution(note that the background hasn't been subtracted).

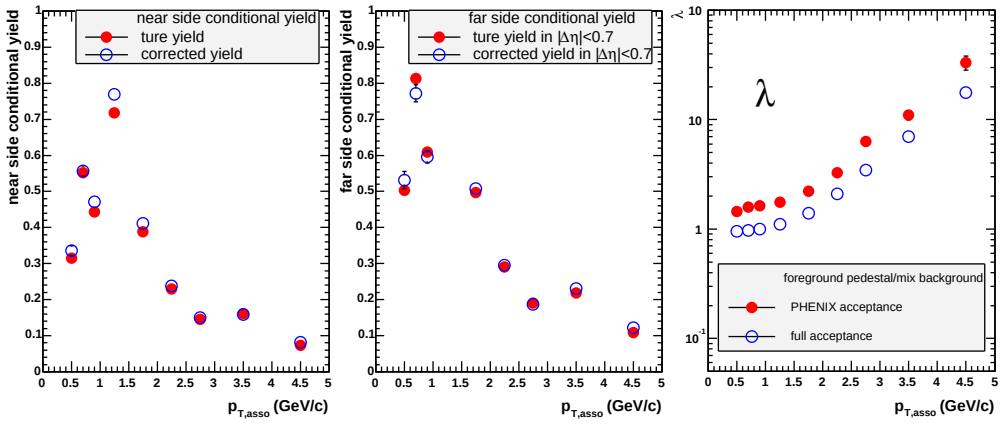

Figure 16: The final corrected yield as function of $p_{T,asso}$ for the near side jet(left panel) and far side jet(middle panel). The expected conditional yield (solid circle) and the fully corrected conditional yield (open circle) are shown for both cases. The yield as function of $p_{T,asso}$ is not smooth because the bin width is changing. In the right panel, the pedestal factor λ are shown for Type a and Type c of acceptance.

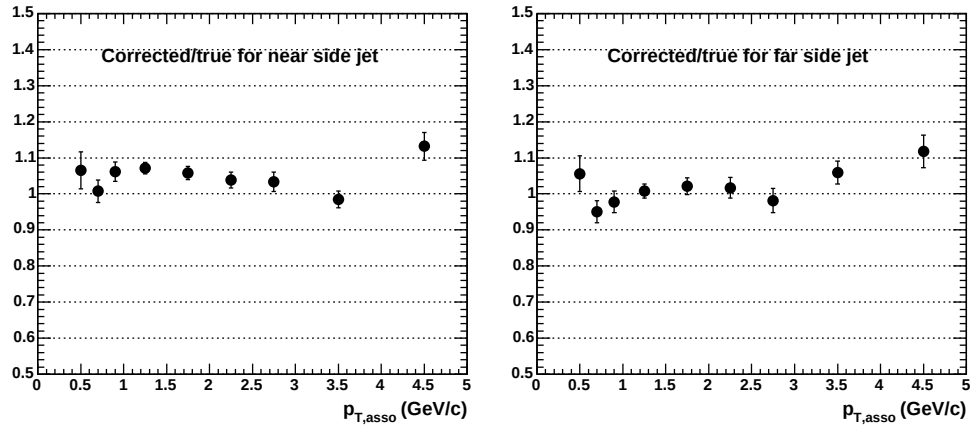

Figure 17: The ratio of the fully corrected conditional yield to the expected conditional yield for the near side jet (left panel) and the far side jet (right panel).

5.4 A few words on the StonyBrook normalization

In Eq.44, the choice of $dN_0^{mix}/d\Delta\phi d\Delta\eta$ to be constant m_0 in some sense is arbitrary, because it appears in both the numerator and the denominator and naturally cancels. Thus we can uses a different definition, and the result should not change.

In ppg033 and several other analysis, people 'correct the yield back into PHENIX acceptance'. What they means is that they already constrains their mixed pairs to be within PHENIX acceptance, so

$$\frac{dN_0^{mix}}{d\Delta\phi d\Delta\eta} = m_0 Acc_1(\Delta\eta) \tag{78}$$

Where Acc_1 is the pair acceptance function in η defined in Eq.46. The sum rule Eq.42 for mixed background has different meaning now. n_b are the multiplicity in $|\eta| < 0.35$ in stead of $|\eta| < 0.7$. For quick reference, we rewrite that equation down here.

$$\int\int d\Delta\phi d\Delta\eta \frac{dN_0^{mix}}{d\Delta\phi d\Delta\eta} = N_{evts} \langle n_a \rangle \langle n_b^{new} \rangle \tag{79}$$

Where we have replace n_b with n_b^{new} and $n_b = 2n_b^{new}$.

This would also means the true mixed background and the measured mixed background have the same triangular shape in $\Delta\eta$, so $I_\eta(I_\eta = 2)$ in Eq.60 drops out pair efficiency Eq.68 becomes

$$\begin{aligned} \epsilon_{asso}^{new} &= \frac{K\prime_{ab}}{R_{\Delta\eta}} \frac{k^{fg}(\Delta\phi)}{k^{mix}(\Delta\phi)} \frac{\langle n\prime_b \rangle}{\langle n_b^{new} \rangle} \\ &\equiv \epsilon_{asso}!!! \end{aligned} \tag{80}$$

Thus the two methods are equivalent.

References

[1] Paul stankus's Analysis note, *https* : *//www.phenix.bnl.gov/phenix/WWW/p/draft/stankus/an*

[2] J.E. Huth *et al.* in *Proceedings of Research Directions For The Decade: Snowmass 1990*, July, 1990, edited by E.L. Berger (World Scientific, Singapore, 1992) p. 134.

[3] S. Catani, Yu.L. Dokshitzer, M.H. Seymour, and B.R. Webber, Nucl. Phys. **B406**, 187 (1993),Phys. Lett. **B285**, 291 (1992); S.D. Ellis and D.E. Soper, Phys. Rev. **D48**, 3160 (1993).

[4] I. Vendramin,Nuovo Cimento **A62**, 21 (1981),Nuovo Cimento **A66**, 339 (1981).

[5] D.Drijard, H.G. Fischer and T. Nakada, Nucl. Instrum. Methods**225**, 367 (1984).

[6] E.L. Berger *et al.* Phys. Rev. **D77**, 206 (1977).

[7] W.A. Zajc *et al.* Phys. Rev. **C29**, 2173 (1984).

[8] D.H. Boal, C.K. Gelbke and B.K. Jennings, Rev. Mod. Phys. **62**, 553 (1990).

[9] W.A. Zajc, Nucl. Phys. **A525**, 315c (1991).

[10] G. Hering, nucl-ex/0203004.

[11] D. L'Hote, Nucl. Instrum. Methods **A337**, 544 (1994).

[12] M. Gazdzicki *et al.* hep-ph/0003319.

[13] Analysis note 116, T.K. Hemmick, et. al, Measurements of Continuum Electron Yield.

[14] B. Lenkeit *et al.* NPA**661**, 23 (1999).

[15] J. Jia and B. Cole, Charged pion R_{cp} in $d-Au$, Analysis note 311.

[16] Ane Sickle, Analysis note 261 and 299.

[17] Mike Reuter, Analysis note 263.

[18] Mickey Chiu's Analysis note, in preparation.

[19] W.G. Holzmann et. al, Analysis note 283.